Markovian models for SAR images: Application to water detection in SWOT satellite images and multi-temporal analysis of urban areas

Sylvain Lobry

PhD defense, 11/16/2017

Financed by **Futur & Ruptures (IMT)** and **CNES**

Thesis advisors:

Roger Fjørtoft Florence Tupin

Co-advisor:

Loïc Denis

Context

- Studies of water dynamics: important topic.
- Spatial data in addition to data acquired on site.

Aerial view of the Amazon river (©lubasi on Flickr).

Context

- Studies of water dynamics: important topic.
- Spatial data in addition to data acquired on site.
- ⇒ **SWOT** mission:
  - NASA-JPL / CNES.
  - Surface Water Ocean Topography
- Will provide global measurements of water elevation:
  - hydrology;
  - oceanography.
- Launch date: April 2021 (planned)

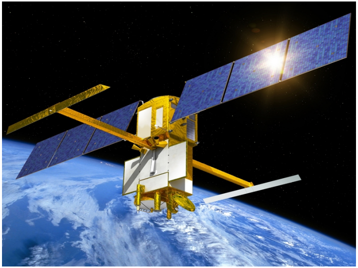

SWOT (©JPL).

Context

Objective

Detect water in SWOT images as a first step towards height estimation.

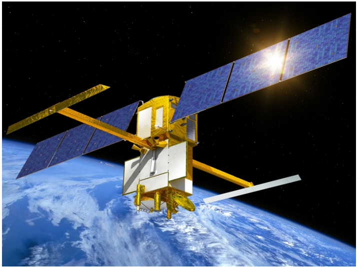

SWOT (©JPL).

SWOT $\Rightarrow$ SAR system:

1. How does SAR work?
2. Particular characteristics of SWOT?

SAR principle

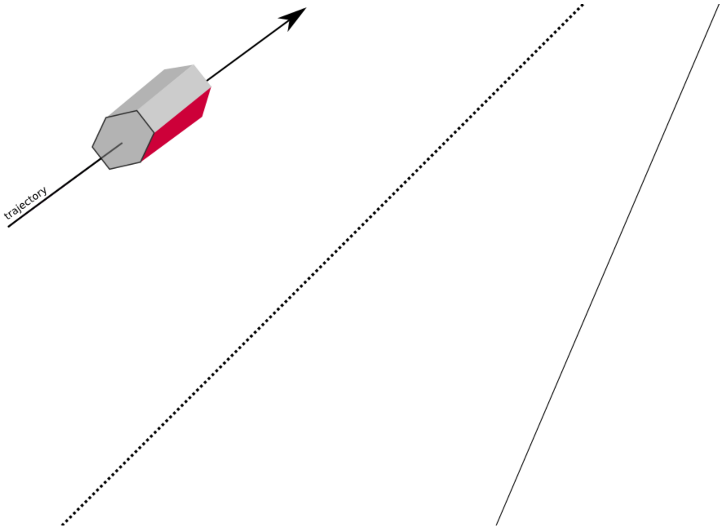

SAR principle

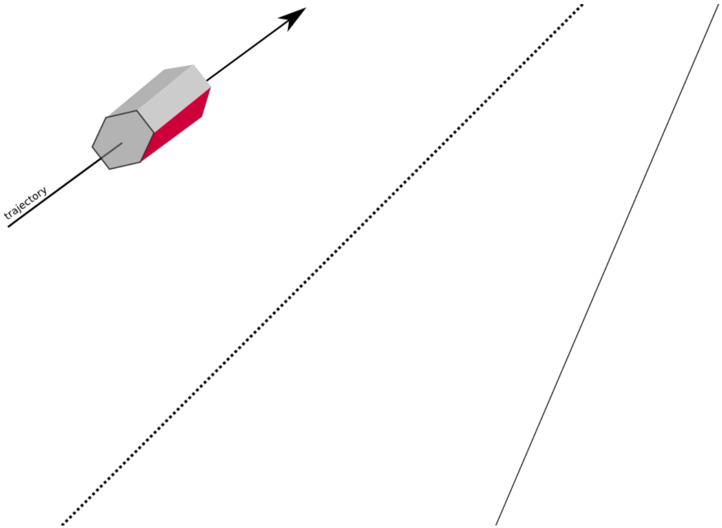

SAR principle

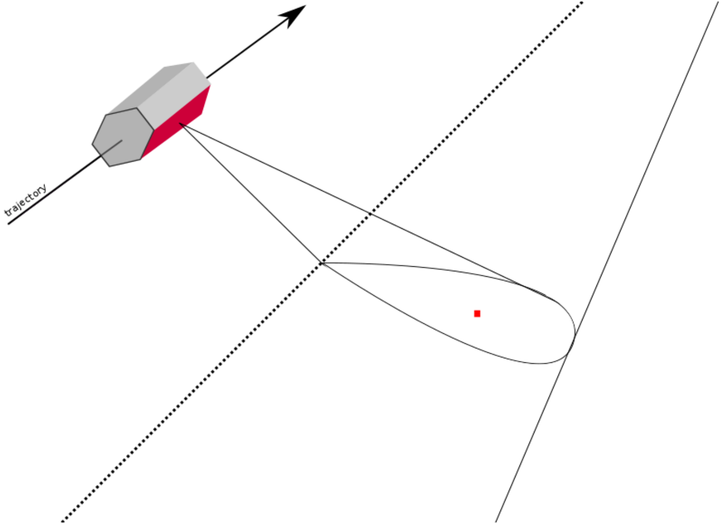

SAR principle

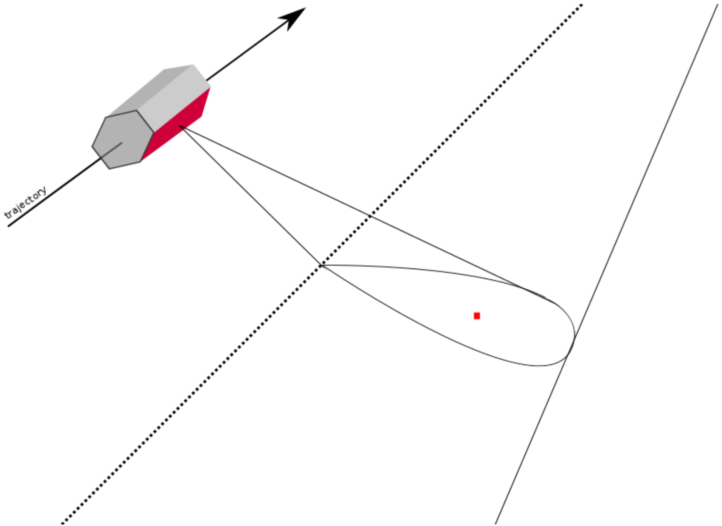

SAR principle

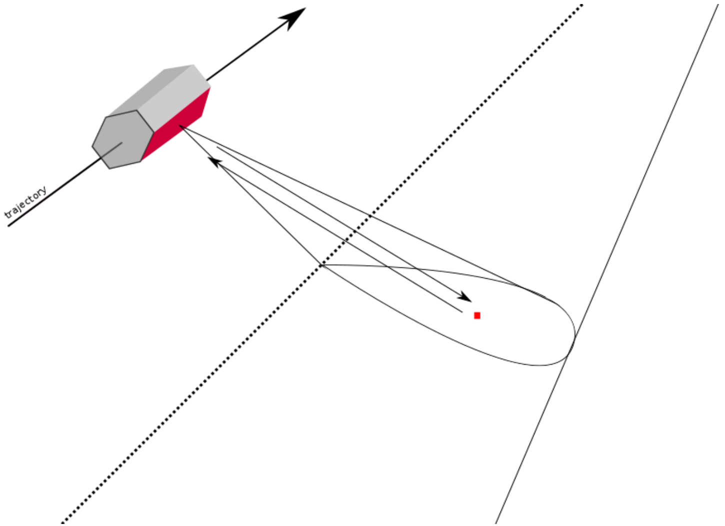

SAR principle

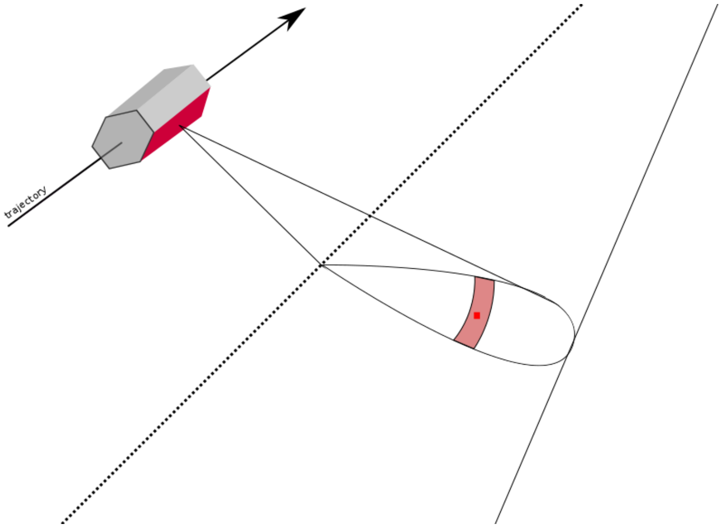

SAR principle

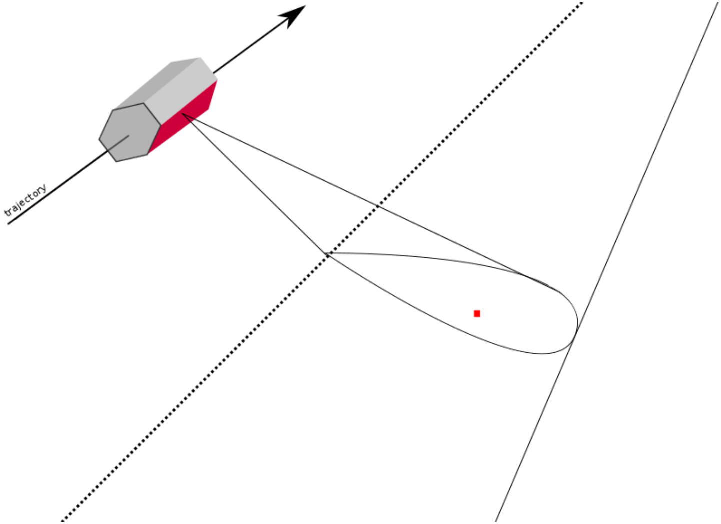

SAR principle

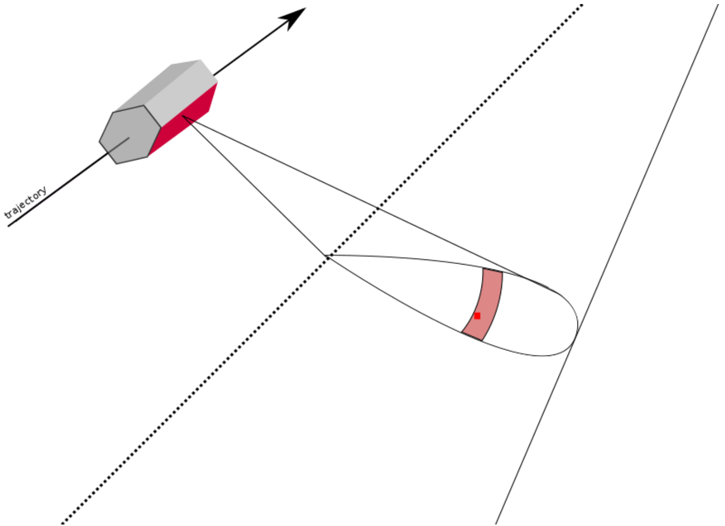

SAR principle

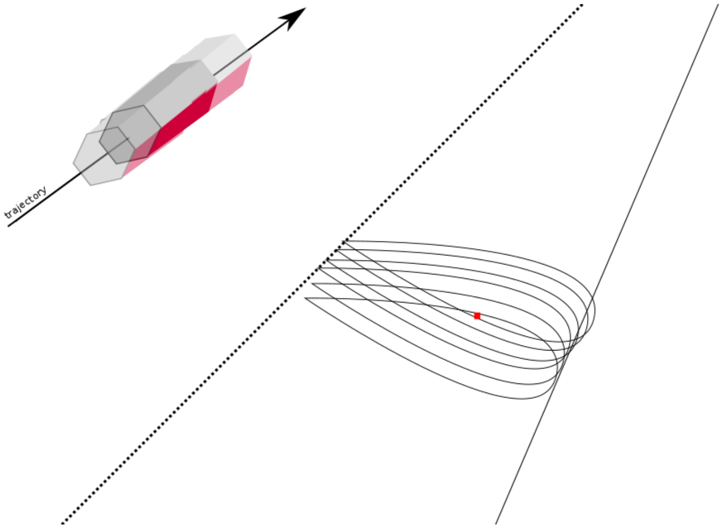

SAR principle

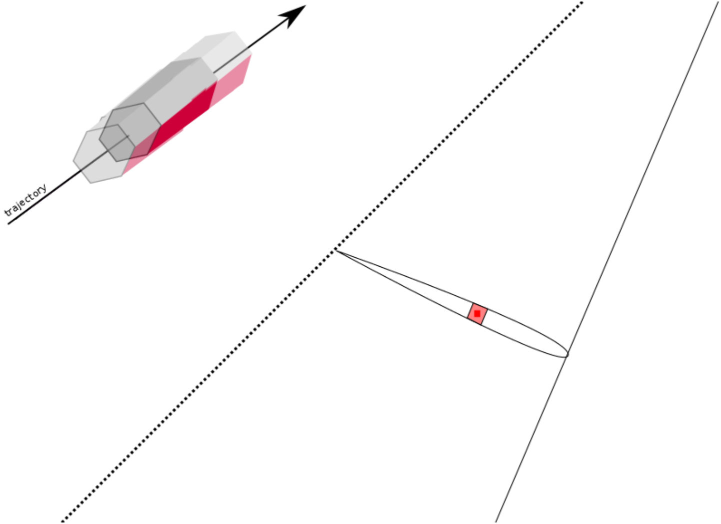

SAR principle

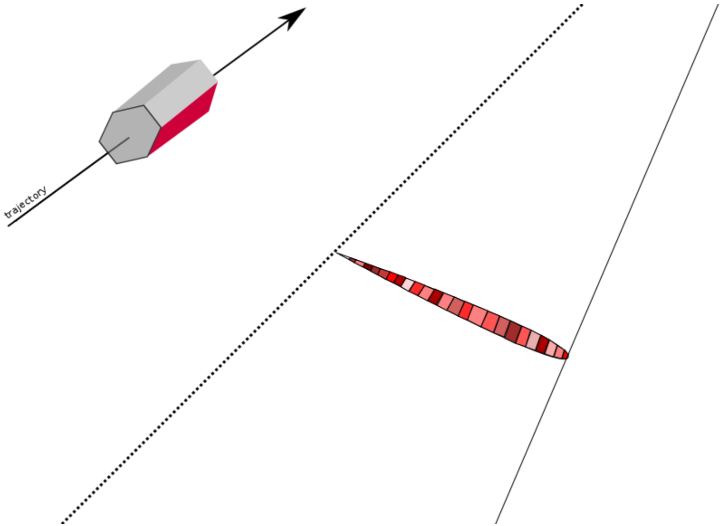

SAR principle

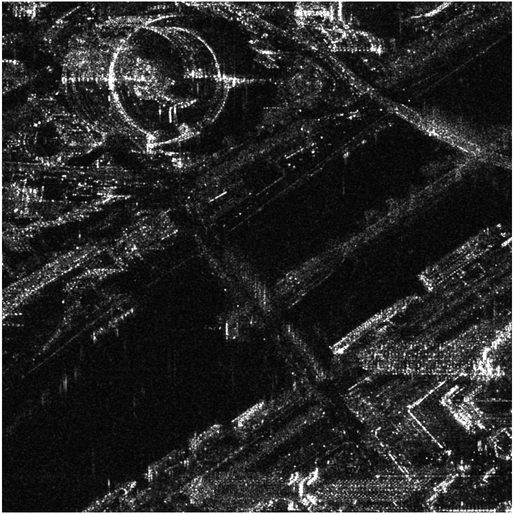

Amplitude image of Paris, acquired by TerraSAR-X

Advantages

- Emits electromagnetic waves (about 1 to 10 GHz).
- Records backscattered signal.
- SAR processing

Advantages

- Emits electromagnetic waves (about 1 to 10 GHz).
- Records backscattered signal.
- SAR processing $\Rightarrow$ Single-look complex images:
  - Amplitude: information on the imaged surface.
  - Phase: height information for 2+ images (interferometry).
  - Polarization: information on the nature of the imaged objects.

Advantages

- Emits electromagnetic waves (about 1 to 10 GHz).
- Records backscattered signal.
- SAR processing $\Rightarrow$ Single-look complex images:
  - Amplitude: information on the imaged surface.
  - Phase: height information for 2+ images (interferometry).
  - Polarization: information on the nature of the imaged objects.

Advantages

- Emits electromagnetic waves (about 1 to 10 GHz).
- Records backscattered signal.
- SAR processing $\Rightarrow$ Single-look complex images:
  - Amplitude: information on the imaged surface.
  - Phase: height information for 2+ images (interferometry).
  - Polarization: information on the nature of the imaged objects.

Advantages

- Emits electromagnetic waves (about 1 to 10 GHz).
- Records backscattered signal.
- SAR processing $\Rightarrow$ Single-look complex images:
  - Amplitude: information on the imaged surface.
  - Phase: height information for 2+ images (interferometry).
  - Polarization: information on the nature of the imaged objects.

Some advantages:

- All-weather.
- Radiometric stability.
- Possibility for polarimetry.
- Possibility for interferometry.

Multi-temporal information

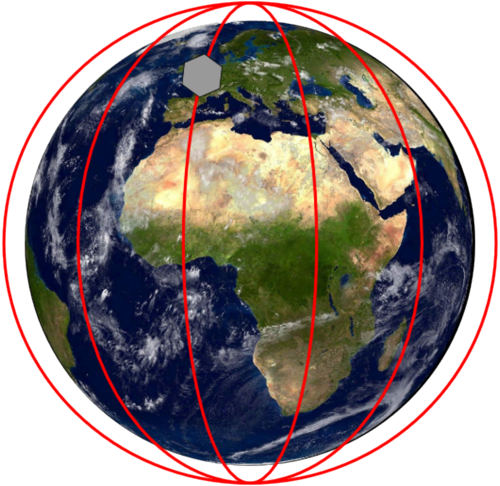

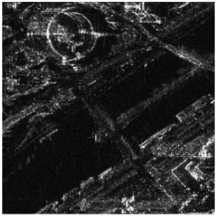

Multi-temporal information

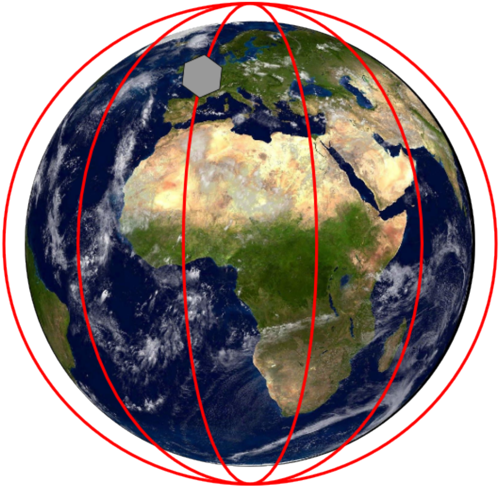

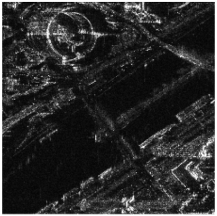

Backscattered signal

- Sensitivity to surface roughness (at the scale of the wavelength):

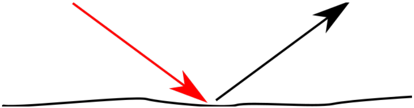

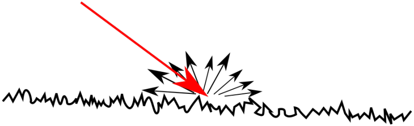

conventional spaceborne SAR on water

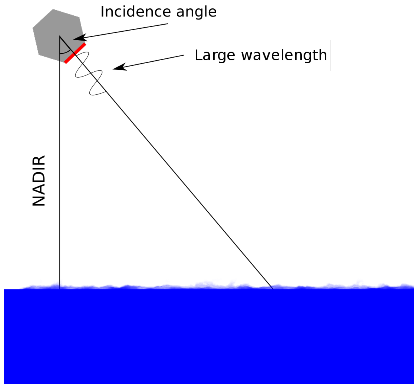

Band	λ (cm)
L	23.6
C	5.55
X	3.11

Incidence angle: $\approx 30^\circ$

conventional spaceborne SAR on water

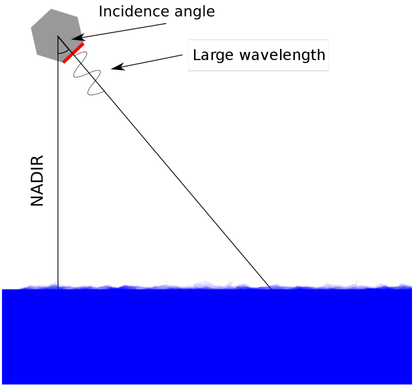

Band	λ (cm)
L	23.6
C	5.55
X	3.11

Incidence angle: $\approx 30^\circ$

conventional spaceborne SAR on water

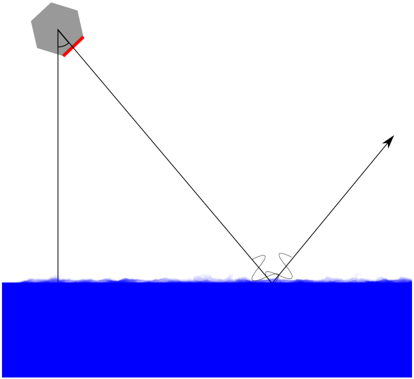

Band	λ (cm)
L	23.6
C	5.55
X	3.11

Incidence angle: $\approx 30^\circ$

Large wavelength (w.r.t. surface water roughness) $\Rightarrow$ specular reflection.
Specular reflection + high incidence angle $\Rightarrow$ no signal received.

conventional spaceborne SAR on water

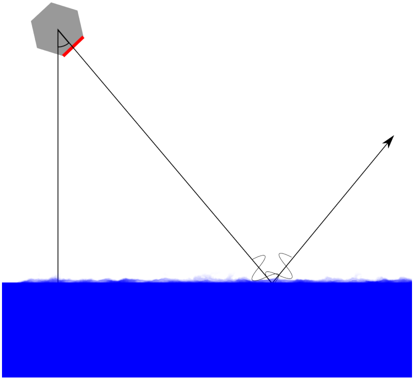

Band	λ (cm)
L	23.6
C	5.55
X	3.11

Incidence angle: $\approx 30^\circ$

Large wavelength (w.r.t. surface water roughness) $\Rightarrow$ specular reflection.
Specular reflection + high incidence angle $\Rightarrow$ no signal received.

SAR on water, Sentinel-1A

Landsat 8 (optic) image

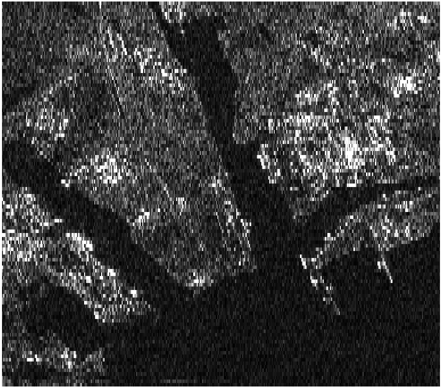

Sentinel-1A (SAR), resampled

Images of the Camargue area, France

SWOT on water

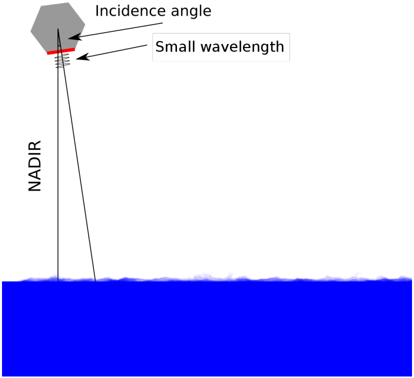

Band	λ (cm)
Ka	0.86

SWOT on water

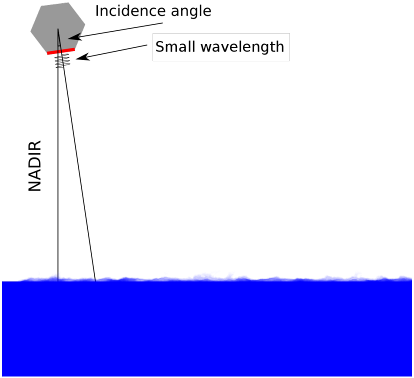

Band	λ (cm)
Ka	0.86

SWOT on water

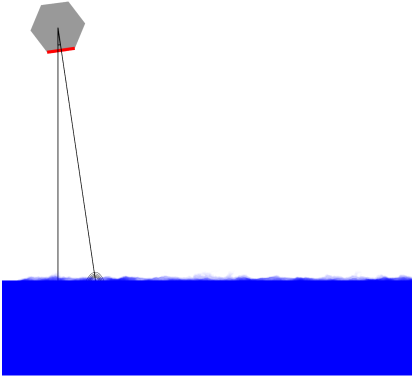

Band	λ (cm)
Ka	0.86

Small wavelength (w.r.t. surface water roughness)
$\Rightarrow$ backscattering not limited to the reflection direction.
+ near-nadir acquisition $\Rightarrow$ Signal received.

SWOT on water

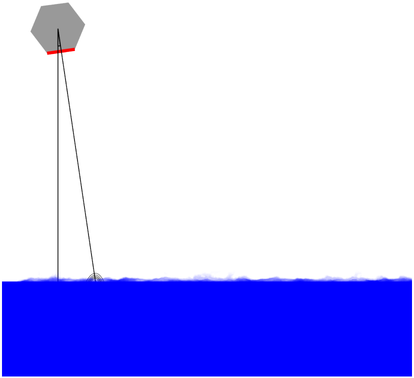

Band	λ (cm)
Ka	0.86

Small wavelength (w.r.t. surface water roughness)
$\Rightarrow$ backscattering not limited to the reflection direction.
+ near-nadir acquisition $\Rightarrow$ Signal received.

SWOT on water

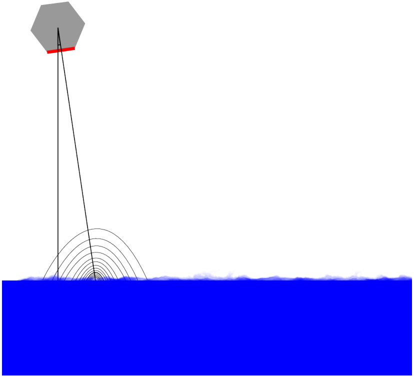

Band	λ (cm)
Ka	0.86

Small wavelength (w.r.t. surface water roughness)

$\Rightarrow$ backscattering not limited to the reflection direction.

+ near-nadir acquisition $\Rightarrow$ Signal received.

However, smooth surface $\Rightarrow$ still no signal.

Reflectivity vs incidence angle

Evolution of the σ_0 (reflectivity coefficient)

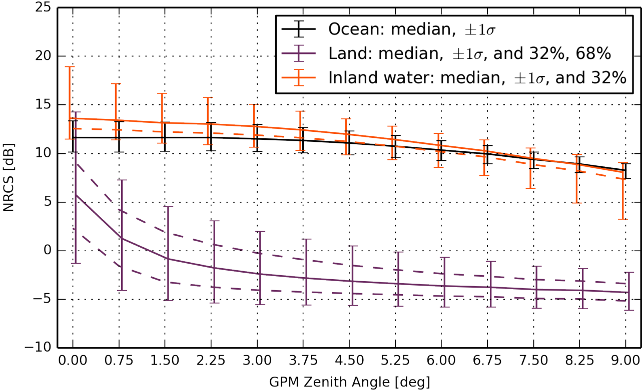

E. Rodriguez, D. Esteban Fernandez, E. Peral, C. Chen, J.-W. De Bleser, and B. A. Williams, "Wide- swath altimetry: A review," in Satellite Altimetry and Earth Sciences 2 (D. Stammer and A. Cazenave, eds.), Chapter 2, CRC Press, 2017.

SAR on water, SWOT

Landsat 8 (optic) image

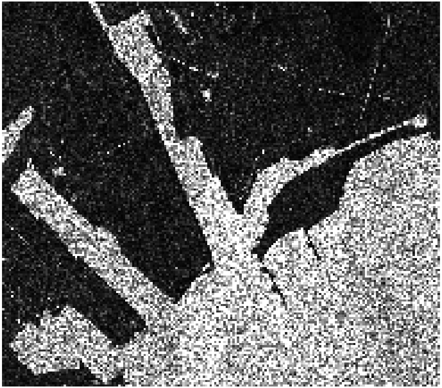

SWOT (SAR)

Images of the Camargue area, France

SAR on water, SWOT

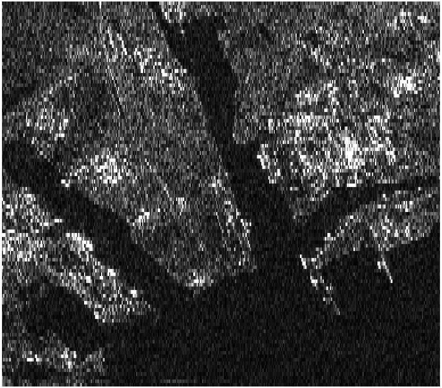

Sentinel-1A (SAR), resampled

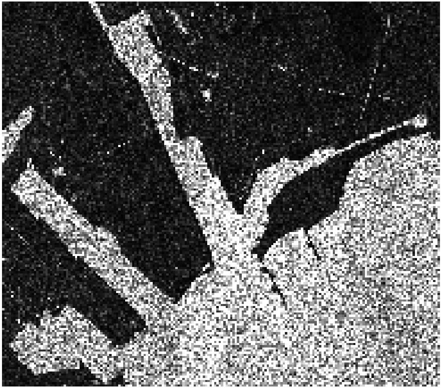

SWOT (SAR)

Images of the Camargue area, France

Particular characteristics of SWOT

- Principal instrument: KaRIn ("Ka-band Radar Interferometer"):
  - Ka-band: f $= 35.75$GHz, $\lambda = 8.6mm$.
  - near-nadir incidence angle: $0.6°$ to $3.9°$.
  - resolution: $5m \times 70m$ to $5m \times 10m$.

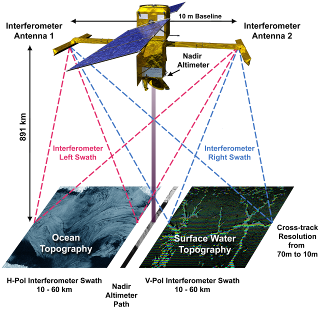

SWOT. (©JPL)

Particular characteristics of SWOT

- Principal instrument: KaRIn ("Ka-band Radar Interferometer"):
  - Ka-band: f $= 35.75$GHz, $\lambda = 8.6mm$.
  - near-nadir incidence angle: 0.6° to 3.9°.
  - resolution: $5m \times 70m$ to $5m \times 10m$.
- Unusual acquisition parameters
  $\Longrightarrow$ unusual image characteristics
  $\Longrightarrow$ calls for new methods.

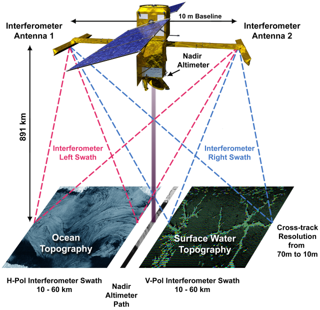

SWOT. (©JPL)

Particular characteristics of SWOT

- Principal instrument: KaRIn ("Ka-band Radar Interferometer"):
  - Ka-band: f $= 35.75$GHz, $\lambda = 8.6mm$.
  - near-nadir incidence angle: $0.6°$ to $3.9°$.
  - resolution: $5m \times 70m$ to $5m \times 10m$.
- Unusual acquisition parameters
  $\Longrightarrow$ unusual image characteristics
  $\Longrightarrow$ calls for new methods.
- Launch planned in April 2021
  $\Rightarrow$ difficult to have realistic and fully representative multi-temporal data
  $\Rightarrow$simulated images

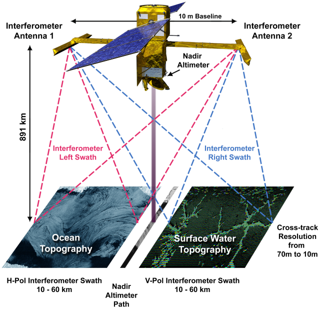

SWOT. (©JPL)

Outline

Part 1
Water detection in SWOT amplitude images

Part 2
Processing of multi-temporal series of SAR images

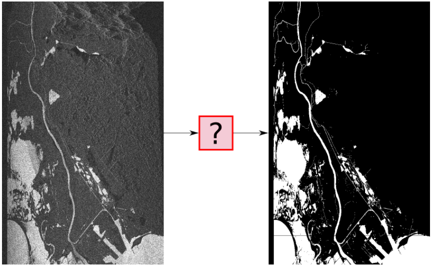

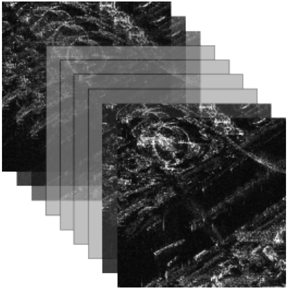

Outline

Part 1
Water detection in SWOT amplitude images

Part 2
Processing of multi-temporal series of SAR images

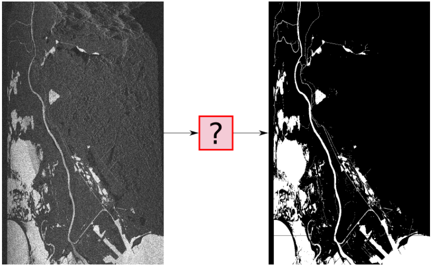

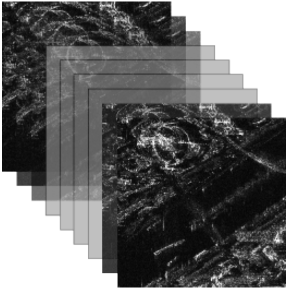

Problem formulation

Observation $\boldsymbol{v}$

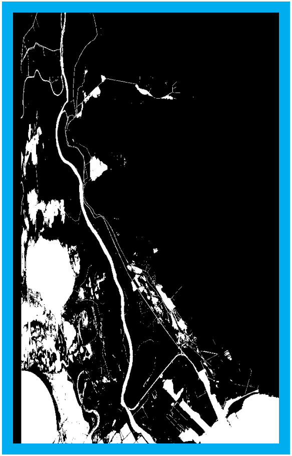

Classification $\boldsymbol{u}$

$$\text{At each pixel } i,\, u_i = \begin{cases} 0 & \text{if land} \\ 1 & \text{if water} \end{cases}$$

with u_i the value of image $\boldsymbol{u}$ at pixel i.

Problem formulation

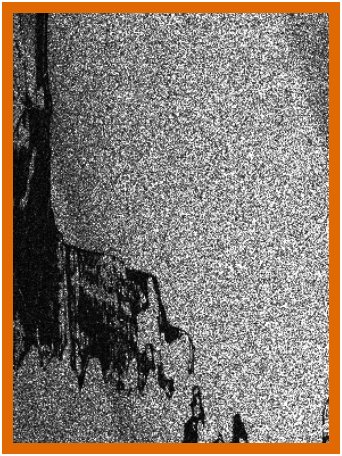

Observation $\boldsymbol{v}$

Classification $\boldsymbol{u}$

$$\text{At each pixel } i, u_i = \begin{cases} 0 & \text{if land} \\ 1 & \text{if water} \end{cases}$$

with u_i the value of image $\boldsymbol{u}$ at pixel i.

Problem formulation using a Bayesian framework

In a Bayesian framework, the MAP classification $\hat{\boldsymbol{u}}$ is given by:

$$\hat{\boldsymbol{u}} = \arg\max_{\boldsymbol{u}} p(\boldsymbol{u}|\boldsymbol{v}) = \arg\max_{\boldsymbol{u}} \frac{p(\boldsymbol{v}|\boldsymbol{u})p(\boldsymbol{u})}{p(\boldsymbol{v})}$$

Problem formulation using a Bayesian framework

In a Bayesian framework, the MAP classification $\hat{u}$ is given by:

$$\hat{u} = \arg\max_{u} p(u|v) = \arg\max_{u} \frac{\underline{p(v|u)}p(u)}{p(v)}$$

- $p(v|u)$ is the likelihood $\Rightarrow$ depends on the physics of the acquisition.

Problem formulation using a Bayesian framework

In a Bayesian framework, the MAP classification $\hat{\boldsymbol{u}}$ is given by:

$$\hat{\boldsymbol{u}} = \arg\max_{\boldsymbol{u}} p(\boldsymbol{u}|\boldsymbol{v}) = \arg\max_{\boldsymbol{u}} \frac{p(\boldsymbol{v}|\boldsymbol{u})\underline{p(\boldsymbol{u})}}{p(\boldsymbol{v})}$$

- $p(\boldsymbol{v}|\boldsymbol{u})$ is the likelihood $\Rightarrow$ depends on the physics of the acquisition.
- $p(\boldsymbol{u})$ is a prior on the desired solution $\Rightarrow$ to be defined by the model.

Problem formulation using a Bayesian framework

In a Bayesian framework, the MAP classification $\hat{\boldsymbol{u}}$ is given by:

$$\hat{\boldsymbol{u}} = \arg\max_{\boldsymbol{u}} p(\boldsymbol{u}|\boldsymbol{v}) = \arg\max_{\boldsymbol{u}} \frac{p(\boldsymbol{v}|\boldsymbol{u})p(\boldsymbol{u})}{\underline{p(\boldsymbol{v})}}$$

- $p(\boldsymbol{v}|\boldsymbol{u})$ is the likelihood $\Rightarrow$ depends on the physics of the acquisition.
- $p(\boldsymbol{u})$ is a prior on the desired solution $\Rightarrow$ to be defined by the model.
- $p(\boldsymbol{v})$ is constant w.r.t. $\boldsymbol{u}$.

Problem formulation using a Bayesian framework

In a Bayesian framework, the MAP classification $\hat{\boldsymbol{u}}$ is given by:

$$\hat{\boldsymbol{u}} = \arg\max_{\boldsymbol{u}} p(\boldsymbol{u}|\boldsymbol{v}) = \arg\max_{\boldsymbol{u}} p(\boldsymbol{v}|\boldsymbol{u})p(\boldsymbol{u})$$

- $p(\boldsymbol{v}|\boldsymbol{u})$ is the likelihood $\Rightarrow$ depends on the physics of the acquisition.
- $p(\boldsymbol{u})$ is a prior on the desired solution $\Rightarrow$ to be defined by the model.
- $p(\boldsymbol{v})$ is constant w.r.t. $\boldsymbol{u}$.

Problem formulation using a Bayesian framework

In a Bayesian framework, the MAP classification $\hat{\boldsymbol{u}}$ is given by:

$$\hat{\boldsymbol{u}} = \arg\max_{\boldsymbol{u}} p(\boldsymbol{u}|\boldsymbol{v}) = \arg\max_{\boldsymbol{u}} \underline{p(\boldsymbol{v}|\boldsymbol{u})}p(\boldsymbol{u})$$

- $p(\boldsymbol{v}|\boldsymbol{u})$ is the likelihood $\Rightarrow$ depends on the physics of the acquisition.
- $p(\boldsymbol{u})$ is a prior on the desired solution $\Rightarrow$ to be defined by the model.
- $p(\boldsymbol{v})$ is constant w.r.t. $\boldsymbol{u}$.

Likelihood definition

We suppose the likelihood of each pixel separable:

$$p(\boldsymbol{v}|\boldsymbol{u}) = \prod_i p(v_i|u_i)$$

Likelihood definition

Coherent imagery $\Rightarrow$ speckle
Fully-developed speckle $\Rightarrow$ multiplicative Rayleigh-Nakagami when considering amplitude [Goodman, 2007]:

$$p(v_i|u_i) = \frac{2\sqrt{L}}{\Gamma(L)\mu_{u_i}} \left(\frac{v_i\sqrt{L}}{\mu_{u_i}}\right)^{2L-1} e^{-\left(\frac{v_i\sqrt{L}}{\mu_{u_i}}\right)^2}.$$

Parameters	
L	Number of looks
μ_{u_i}	reflectivity

- $L = 1$ (no pre-filtering):

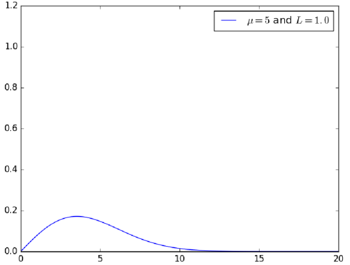

Likelihood definition

Coherent imagery ⇒ speckle
Fully-developed speckle ⇒ multiplicative Rayleigh-Nakagami when considering amplitude [Goodman, 2007]:

$$p(v_i|u_i) = \frac{2\sqrt{L}}{\Gamma(L)\mu_{u_i}}\left(\frac{v_i\sqrt{L}}{\mu_{u_i}}\right)^{2L-1} e^{-\left(\frac{v_i\sqrt{L}}{\mu_{u_i}}\right)^2}.$$

Parameters	
L	Number of looks
μ_{u_i}	reflectivity

- $L = 1$ (no pre-filtering):

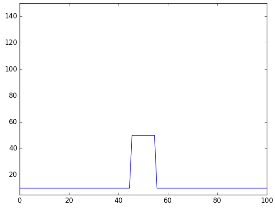

Input signal

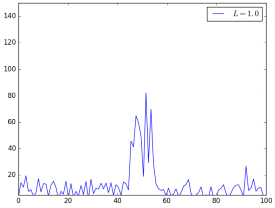

Multiplicative Rayleigh ($L = 1$).

Likelihood definition

Coherent imagery ⇒ speckle
Fully-developed speckle ⇒ multiplicative Rayleigh-Nakagami when considering amplitude [Goodman, 2007]:

$$p(v_i|u_i) = \frac{2\sqrt{L}}{\Gamma(L)\mu_{u_i}} \left(\frac{v_i\sqrt{L}}{\mu_{u_i}}\right)^{2L-1} e^{-\left(\frac{v_i\sqrt{L}}{\mu_{u_i}}\right)^2}.$$

Parameters	
L	Number of looks
μ_{u_i}	reflectivity

- $L = 1$ (no pre-filtering):

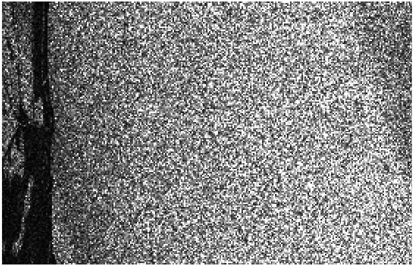

Likelihood definition

Coherent imagery $\Rightarrow$ speckle
Fully-developed speckle $\Rightarrow$ multiplicative Rayleigh-Nakagami when considering amplitude [Goodman, 2007]:

$$p(v_i|u_i) = \frac{2\sqrt{L}}{\Gamma(L)\mu_{u_i}} \left(\frac{v_i\sqrt{L}}{\mu_{u_i}}\right)^{2L-1} e^{-\left(\frac{v_i\sqrt{L}}{\mu_{u_i}}\right)^2}.$$

Parameters	
L	Number of looks
μ_{u_i}	reflectivity

- Multi-looking: spatial (or temporal) average

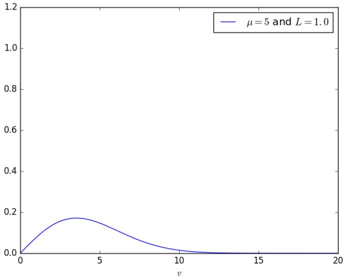

Likelihood definition

Coherent imagery ⇒ speckle
Fully-developed speckle ⇒ multiplicative Rayleigh-Nakagami when considering amplitude [Goodman, 2007]:

$$p(v_i|u_i) = \frac{2\sqrt{L}}{\Gamma(L)\mu_{u_i}} \left(\frac{v_i\sqrt{L}}{\mu_{u_i}}\right)^{2L-1} e^{-\left(\frac{v_i\sqrt{L}}{\mu_{u_i}}\right)^2}.$$

	Parameters
L	Number of looks
μ_{u_i}	reflectivity

- Multi-looking: spatial (or temporal) average

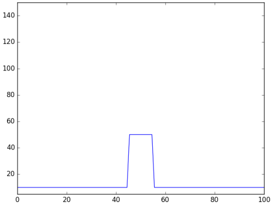

Input signal

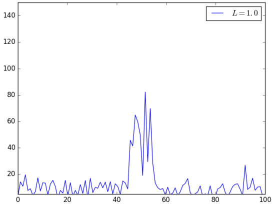

Multiplicative Rayleigh.

Prior definition

In a Bayesian framework, classification $\hat{\boldsymbol{u}}$ is given by:

$$\hat{\boldsymbol{u}} = \arg\max_{\boldsymbol{u}} p(\boldsymbol{u}|\boldsymbol{v}) = p(\boldsymbol{v}|\boldsymbol{u})\underline{p(\boldsymbol{u})}$$

- $p(\boldsymbol{v}|\boldsymbol{u})$ is the likelihood $\Rightarrow$ depends on the physics of the acquisition.
- $p(\boldsymbol{u})$ is a prior on the desired solution $\Rightarrow$ to be defined by the model.

Prior definition

p($\boldsymbol{u}$) is considered separable for each pixel and can:

- be constant and equal for each class: $\forall i,\ p(u_i = 0) = p(u_i = 1) = \frac{1}{2}$
- be constant: $\forall i,\ p(u_i = 0) = x$ and $p(u_i = 1) = (1 - x)$
- enforce spatial properties

In this case,

$$\hat{\boldsymbol{u}} = \arg\max_{\boldsymbol{u}} p(\boldsymbol{u}|\boldsymbol{v}) = \arg\max_{\boldsymbol{u}} p(\boldsymbol{v}|\boldsymbol{u})p(\boldsymbol{u}) = \arg\max_{\boldsymbol{u}} p(\boldsymbol{v}|\boldsymbol{u})$$

Separable likelihood $\Rightarrow$ threshold.

Prior definition

p($\boldsymbol{u}$) is considered separable for each pixel and can:

- be constant and equal for each class: $\forall i,\ p(u_i = 0) = p(u_i = 1) = \frac{1}{2}$
- be constant: $\forall i,\ p(u_i = 0) = x$ and $p(u_i = 1) = (1 - x)$
- enforce spatial properties

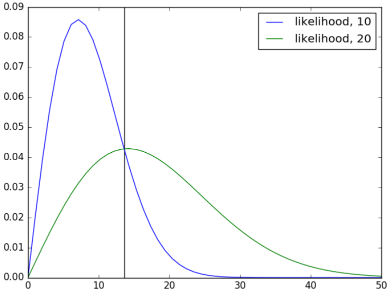

Threshold for $\mu_0 = 10$ and $\mu_1 = 20$

Prior definition

p($\boldsymbol{u}$) is considered separable for each pixel and can:

- be constant and equal for each class: $\forall i,\ p(u_i = 0) = p(u_i = 1) = \frac{1}{2}$
- be constant: $\forall i,\ p(u_i = 0) = x$ and $p(u_i = 1) = (1 - x)$
- enforce spatial properties

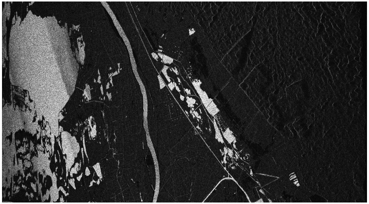

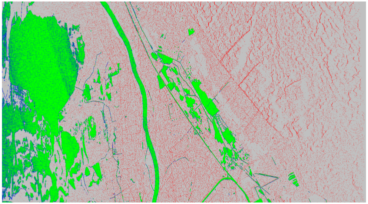

True positive | True negative | False positive | False negative

Prior definition

p($\boldsymbol{u}$) is considered separable for each pixel and can:

- be constant and equal for each class: $\forall i,\ p(u_i = 0) = p(u_i = 1) = \frac{1}{2}$
- be constant: $\forall i,\ p(u_i = 0) = x \text{ and } p(u_i = 1) = 1 - x$
- enforce spatial properties

It is a weighted threshold.
Inland water accounts for 2.5% of the surface:

- $\forall i,\ p(u_i = 0) = 0.975$
- $\forall i,\ p(u_i = 1) = 0.025$

Prior definition

p($\boldsymbol{u}$) is considered separable for each pixel and can:

- be constant and equal for each class: $\forall i,\ p(u_i = 0) = p(u_i = 1) = \frac{1}{2}$
- be constant: $\forall i,\ p(u_i = 0) = x$ and $p(u_i = 1) = 1 - x$
- enforce spatial properties

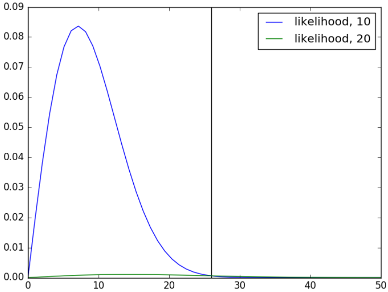

Threshold for $\mu_0 = 10$ and $\mu_1 = 20$

Prior definition

p($\boldsymbol{u}$) is considered separable for each pixel and can:

- be constant and equal for each class: $\forall i,\ p(u_i = 0) = p(u_i = 1) = \frac{1}{2}$
- be constant: $\forall i,\ p(u_i = 0) = x$ and $p(u_i = 1) = 1 - x$
- enforce spatial properties

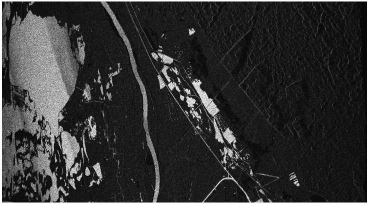

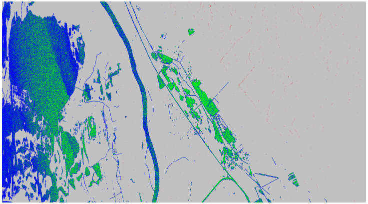

True positive | True negative | False positive | False negative

Prior definition

p($\boldsymbol{u}$) is considered separable for each pixel and can:

- be constant and equal for each class: $\forall i,\ p(u_i = 0) = p(u_i = 1) = \frac{1}{2}$
- be constant: $\forall i,\ p(u_i = 0) = x \text{ and } p(u_i = 1) = (1 - x)$
- enforce spatial properties

Enforcing compactness

Different approaches:

- Denoising before classification.

Main idea: denoising reduces variations of the speckle
$\Rightarrow$ pixel-based classification possible.

- [Liu and Jezek, 2004]: Lee filter [Lee, 1981] (local)
- [Cazals et al., 2016]: Perona-Malik filter [Perona and Malik, 1990] (anisotrope)
- [Cao et al., 2011]: Multi scaling.
- Non-local approaches (e.g. [Deledalle et al., 2015]) could be used.

Enforcing compactness

Different approaches:

- Denoising before classification.
- Segmentation before classification.

Main idea: segment in homogeneous regions
$\Rightarrow$ easier classification.

- Edge detection adapted to SAR [Touzi et al., 1988, Fjørtoft et al., 1998].
- Level-set [Ben Ayed et al., 2005].
- Active contours [Silveira et al., 2009].

Enforcing compactness

Different approaches:

- Denoising before classification.
- Segmentation before classification.
- Markov Random Fields

Markov Random Fields

- Energy:

$$\begin{aligned}\hat{\boldsymbol{u}} &= \arg\max_{\boldsymbol{u}} p(\boldsymbol{u}|\boldsymbol{v}) \\ &= \arg\max_{\boldsymbol{u}} p(\boldsymbol{v}|\boldsymbol{u})p(\boldsymbol{u}) \\ &= \arg\min_{\boldsymbol{u}} -\log(p(\boldsymbol{v}|\boldsymbol{u})) - \log(p(\boldsymbol{u})) \\ &= \arg\min_{\boldsymbol{u}} \mathcal{E}(\boldsymbol{u}) = \sum_i \mathrm{DT}(v_i|u_i) + \beta \sum_{i\sim j} \psi(u_i, u_j)\end{aligned}$$

$i \sim j \Rightarrow i$ and j are neighbor pixels

Simulated SWOT amplitude image ($\boldsymbol{v}$).

Markov Random Fields

- Energy:

$$\hat{\boldsymbol{u}} = \arg\min_{\boldsymbol{u}} \mathcal{E}(\boldsymbol{u}) = \sum_i \mathrm{DT}(v_i|u_i) + \beta \sum_{i\sim j} \psi(u_i, u_j)$$

$i \sim j \Rightarrow i$ and j are neighbor pixels

- Data term (in amplitude) [Goodman, 2007]:

$$\mathrm{DT}(v_i|u_i) = -\log(p(v_i|u_i))$$
$$= 2\log(\mu_{u_i}) + \frac{{v_i}^2}{\mu_{u_i}^2},$$

with μ_{u_i} the local reflectivity at pixel i given the class u_i.

Simulated SWOT amplitude image ($\boldsymbol{v}$).

Markov Random Fields

- Energy:

$$\hat{\boldsymbol{u}} = \arg\min_{\boldsymbol{u}} \mathcal{E}(\boldsymbol{u}) = \sum_i \mathrm{DT}(v_i|u_i) + \beta \sum_{i\sim j} \psi(u_i, u_j)$$

$i \sim j \Rightarrow i$ and j are neighbor pixels

- Prior: Ising model on neighbors:

$$\psi(a,b) = \begin{cases} 1 & \text{if } a \neq b \\ 0 & \text{if } a = b \end{cases}$$

Simulated SWOT amplitude image ($\boldsymbol{v}$).

Markov Random Fields

- Energy:

$$\hat{\boldsymbol{u}} = \arg\min_{\boldsymbol{u}} \mathcal{E}(\boldsymbol{u}) = \sum_i \mathrm{DT}(v_i|u_i) + \beta \sum_{i \sim j} \psi(u_i, u_j)$$

$i \sim j \Rightarrow i$ and j are neighbor pixels

- β tunes the regularization level.

Simulated SWOT amplitude image ($\boldsymbol{v}$).

Markov Random Fields

- Energy:

$$\hat{\boldsymbol{u}} = \arg\min_{\boldsymbol{u}} \mathcal{E}(\boldsymbol{u}) = \sum_i \mathrm{DT}(v_i|u_i) + \beta \sum_{i\sim j} \psi(u_i, u_j)$$

$i \sim j \Rightarrow i$ and j are neighbor pixels

- Optimization: ICM, simulated annealing, graphcuts.

Simulated SWOT amplitude image ($\boldsymbol{v}$).

Graphcut optimization

$$\mathcal{E}(\boldsymbol{u}) = \sum_i \mathrm{DT}(v_i|u_i) + \beta \sum_{i\sim j} \psi(u_i, u_j)$$

with:

$$\psi(a,b) = \begin{cases} 1 & \text{si } a \neq b \\ 0 & \text{si } a = b \end{cases}$$

Finding minimum of $\mathcal{E}(\boldsymbol{u}) \iff$ finding the minimum cut in:

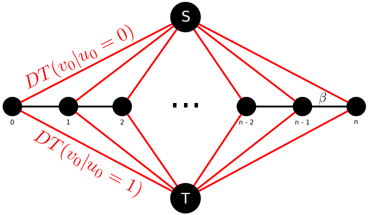

Graph construction for the optimization of the Ising model (here in the 1D case). [Greig et al., 1989]

Results

v

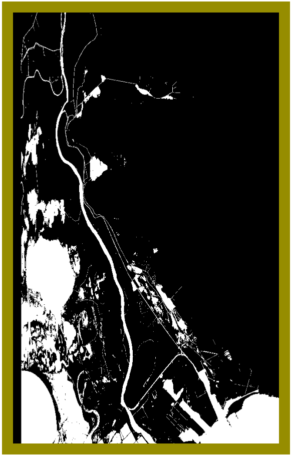

Ground truth

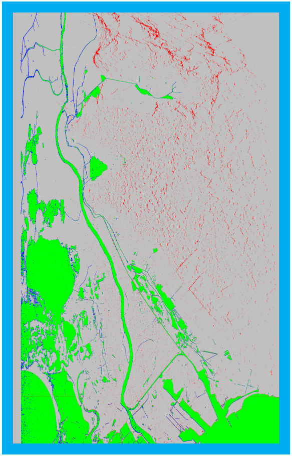

u

True positive | True negative | False positive | False negative

Problem

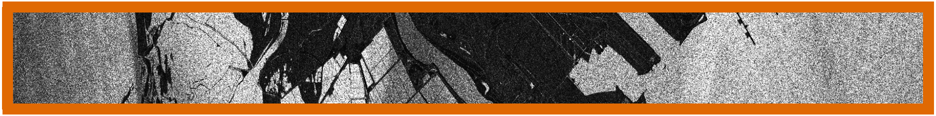

v

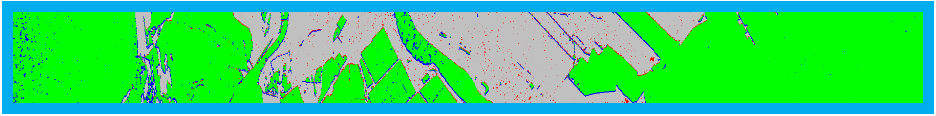

u

Problem

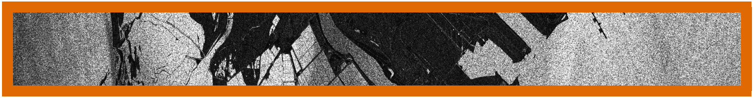

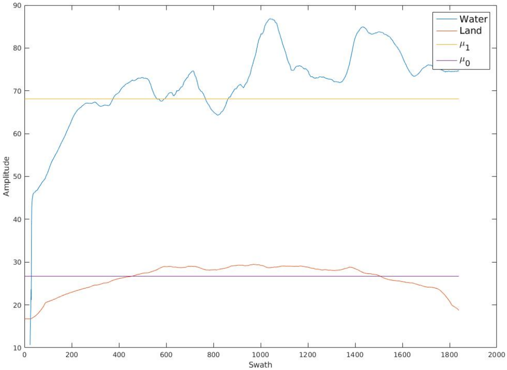

Average evolution of the radiometry parameters of each class through swath and MLE of a constant reflectivity.

Problem

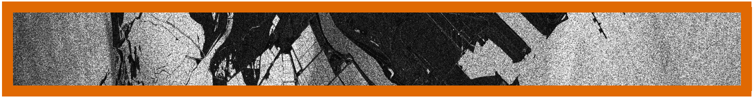

Local variations in surface roughness (wind, turbulence. . .) or slope (topography)

Problem

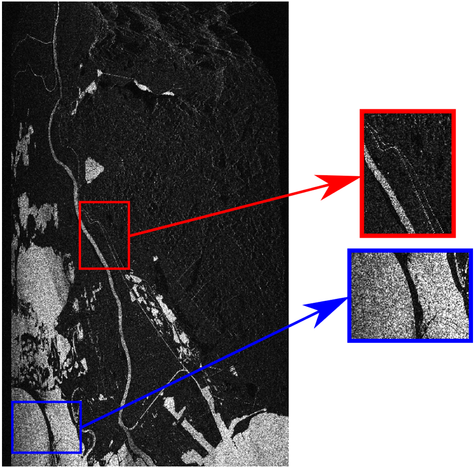

Problem

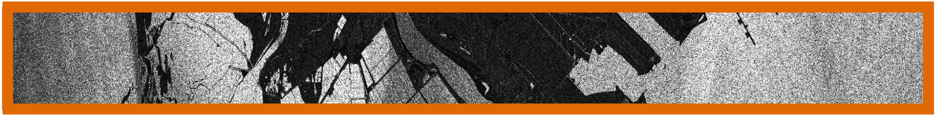

v

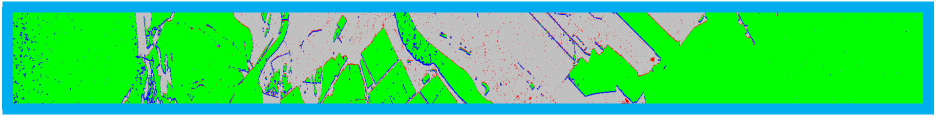

u

SWOT water detection toolchain

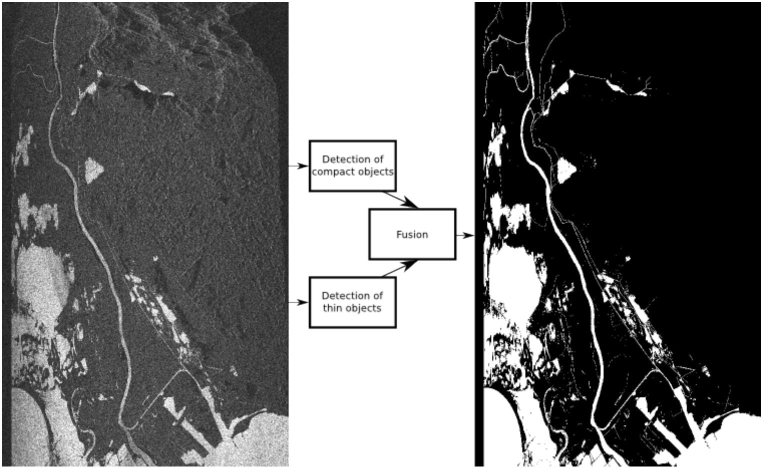

SWOT water detection toolchain

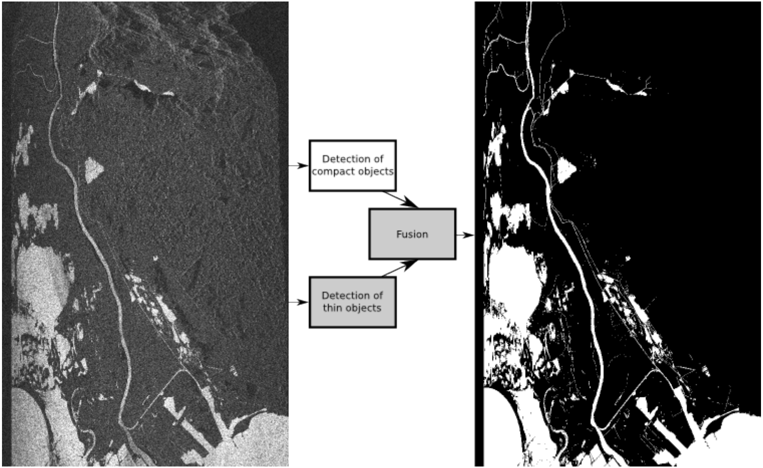

Variable parameters

$$\mathrm{DT}(v_i, u_i) = 2\log(\mu_{u_i}) + \frac{{v_i}^2}{\mu_{u_i}^2}$$

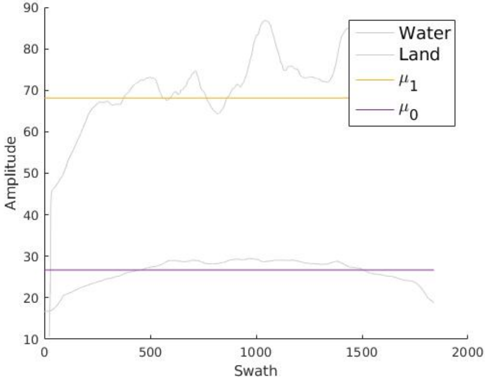

Variable parameters

$$\mathrm{DT}(v_i, u_i) = 2\log(\mu_{u_i}) + \frac{{v_i}^2}{\mu_{u_i}^2}$$

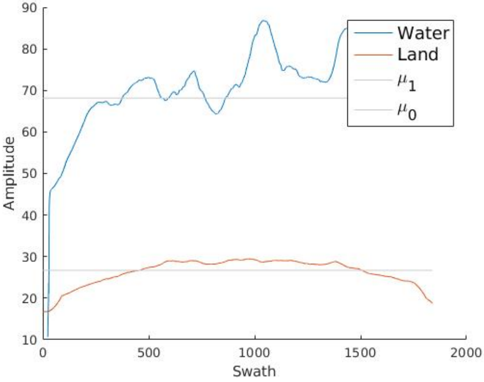

Proposed model

Four random fields:

v observation	u classification	μ parameter maps	μ^0 initial parameter maps

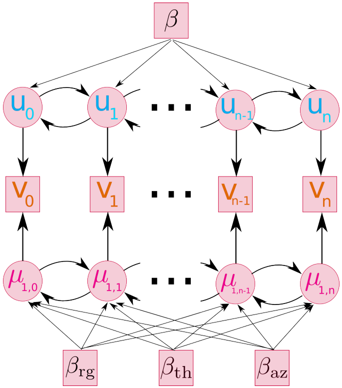

Graphical representation of the dependencies between variables in the 1D case.

Proposed model

Four random fields:

$\boldsymbol{v}$ observation	$\boldsymbol{u}$ classification	$\boldsymbol{\mu}$ parameter maps	$\boldsymbol{\mu}^0$ initial parameter maps

With $\log(x) = \widetilde{x}$:

$$
\begin{aligned}
\mathcal{E}_{\mathrm{MRF2}}(\boldsymbol{u}) = & \sum_i \mathrm{DT}(v_i | u_i, \mu_{1,i}, \mu_{0,i}) \\
& + \beta \sum_{i \sim j} \psi(u_i, u_j) \\
& + \beta_{rg} \sum_{(i,j) \in \mathcal{N}_{\mathrm{rg}}} (\widetilde{\mu_{0,i}} - \widetilde{\mu_{0,j}})^2 + \beta_{az} \sum_{(i,j) \in \mathcal{N}_{\mathrm{az}}} (\widetilde{\mu_{0,i}} - \widetilde{\mu_{0,j}})^2 + \beta_{th} \sum_i (\widetilde{\mu_{0,i}} - \widetilde{\mu^0_{0,i}})^2 \\
& + \beta_{rg} \sum_{(i,j) \in \mathcal{N}_{\mathrm{rg}}} (\widetilde{\mu_{1,i}} - \widetilde{\mu_{1,j}})^2 + \beta_{az} \sum_{(i,j) \in \mathcal{N}_{\mathrm{az}}} (\widetilde{\mu_{1,i}} - \widetilde{\mu_{1,j}})^2 + \beta_{th} \sum_i (\widetilde{\mu_{1,i}} - \widetilde{\mu^0_{1,i}})^2
\end{aligned}
$$

Proposed toolchain

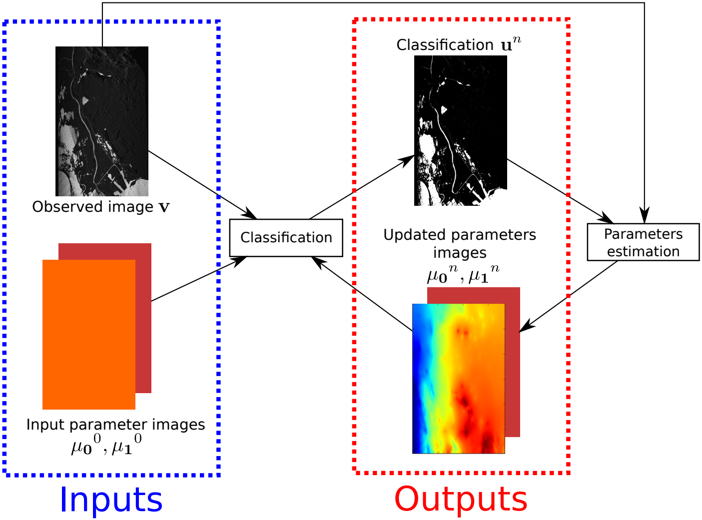

Parameter estimation

To obtain the water parameter map at n^{th} iteration μ_1^n:

- use the observed value for pixel i *iff* $u_i^n = 1$;
- neighbor pixels should have close values;
- it should be close to the initial solution (i.e. theoretical parameters);

$\mu_1^n \sim$ Nakagami $\Rightarrow \widetilde{\mu_1^n} \sim$ Fisher-Tipett $\simeq$ Normal (where $\log(x) = \widetilde{x}$).

Parameter estimation

To obtain the water parameter map at n^{th} iteration μ_1^n:

- use the observed value for pixel i *iff* $u_i^n = 1$;
- neighbor pixels should have close values;
- it should be close to the initial solution (i.e. theoretical parameters);

$\mu_1^n \sim$ Nakagami $\Rightarrow \widetilde{\mu_1^n} \sim$ Fisher-Tipett $\simeq$ Normal (where $\log(x) = \widetilde{x}$).

$$\mathcal{E}_{param}(\widetilde{\mu_1^n}) = \sum_i u_i^n (\widetilde{\mu_{1,i}^n} - \widetilde{v_i})^2$$

Parameter estimation

To obtain the water parameter map at n^{th} iteration μ_1^n:

- use the observed value for pixel i *iff* $u_i^n = 1$;
- neighbor pixels should have close values;
- it should be close to the initial solution (i.e. theoretical parameters);

$\mu_1^n \sim$ Nakagami $\Rightarrow \widetilde{\mu_1^n} \sim$ Fisher-Tipett $\simeq$ Normal (where $\log(x) = \widetilde{x}$).

$$\mathcal{E}_{param}(\widetilde{\mu_1^n}) = \sum_i u_i^n (\widetilde{\mu_{1,i}^n} - \widetilde{v_i})^2$$

$$+ \beta_{rg} \sum_{(i,j)\in\mathcal{N}_{\mathrm{rg}}} (\widetilde{\mu_{1,i}^n} - \widetilde{\mu_{1,j}^n})^2$$ spatial regularization for **range** direction.

$$+ \beta_{az} \sum_{(i,j)\in\mathcal{N}_{\mathrm{az}}} (\widetilde{\mu_{1,i}^n} - \widetilde{\mu_{1,j}^n})^2$$ spatial regularization for **azimuth** direction.

Parameter estimation

To obtain the water parameter map at n^{th} iteration μ_1^n:

- use the observed value for pixel i *iff* $u_i^n = 1$;
- neighbor pixels should have close values;
- it should be close to the initial solution (i.e. theoretical parameters);

$\mu_1^n \sim$ Nakagami $\Rightarrow \widetilde{\mu_1^n} \sim$ Fisher-Tipett $\simeq$ Normal (where $\log(x) = \widetilde{x}$).

$$\mathcal{E}_{param}(\widetilde{\mu_1^n}) = \sum_i u_i^n(\widetilde{\mu_{1,i}^n} - \widetilde{v}_i)^2$$

$$+ \beta_{rg} \sum_{(i,j)\in\mathcal{N}_{\mathrm{rg}}} (\widetilde{\mu_{1,i}^n} - \widetilde{\mu_{1,j}^n})^2$$ spatial regularization for **range** direction.

$$+ \beta_{az} \sum_{(i,j)\in\mathcal{N}_{\mathrm{az}}} (\widetilde{\mu_{1,i}^n} - \widetilde{\mu_{1,j}^n})^2$$ spatial regularization for **azimuth** direction.

$$+ \beta_{th} \sum_i (\widetilde{\mu_{1,i}^n} - \widetilde{\mu_{1,i}^0})^2$$ regularization with respect to initialization (theoretical parameters).

Parameter estimation

To obtain the water parameter map at n^{th} iteration μ_1^n:

- use the observed value for pixel i *iff* $u_i^n = 1$;
- neighbor pixels should have close values;
- it should be close to the initial solution (i.e. theoretical parameters);

$\mu_1^n \sim$ Nakagami $\Rightarrow \widetilde{\mu_1^n} \sim$ Fisher-Tipett $\simeq$ Normal (where $\log(x) = \widetilde{x}$).

$$\mathcal{E}_{param}(\widetilde{\mu_1^n}) = \sum_i u_i^n (\widetilde{\mu_{1,i}^n} - \widetilde{v}_i)^2$$

$$+ \beta_{rg} \sum_{(i,j) \in \mathcal{N}_{\mathrm{rg}}} (\widetilde{\mu_{1,i}^n} - \widetilde{\mu_{1,j}^n})^2$$ spatial regularization for **range** direction.

$$+ \beta_{az} \sum_{(i,j) \in \mathcal{N}_{\mathrm{az}}} (\widetilde{\mu_{1,i}^n} - \widetilde{\mu_{1,j}^n})^2$$ spatial regularization for **azimuth** direction.

$$+ \beta_{th} \sum_i (\widetilde{\mu_{1,i}^n} - \widetilde{\mu_{1,i}^0})^2$$ regularization with respect to initialization (theoretical parameters).

Quadratic function $\Rightarrow$ optimized using conjugate gradient.

Results

Camargue Po Kaw

v

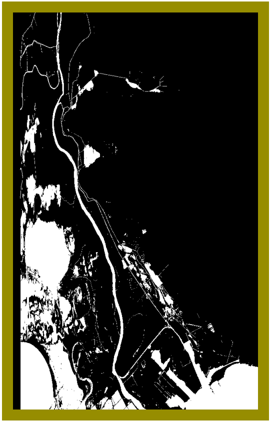

Ground truth

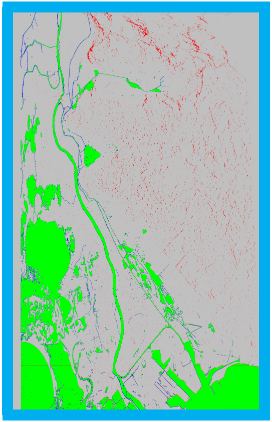

u

True positive True negative False positive False negative

Results

Camargue Po Kaw

	ML	MAP	MRF Constant	Proposed model
TPR	83.26%	39.94%	91.27%	92.78%
FPR	7.54%	0.32%	2.11%	1.64%
MCC	0.70	0.58	0.88	0.91
ER	54.85%	61.69%	19.41%	15.52%

$$\text{True positive rate: TPR} = \frac{TP}{TP + FN}$$

$$\text{False positive rate: FPR} = \frac{FP}{FP + TN}$$

$$\text{MCC} = \frac{TP \times TN - FP \times FN}{\sqrt{(TP + FP)(TP + FN)(TN + FP)(TN + FN)}}$$

$$\text{Error rate: ER} = \frac{FP + FN}{TP + FN}$$

Results

Camargue Po Kaw

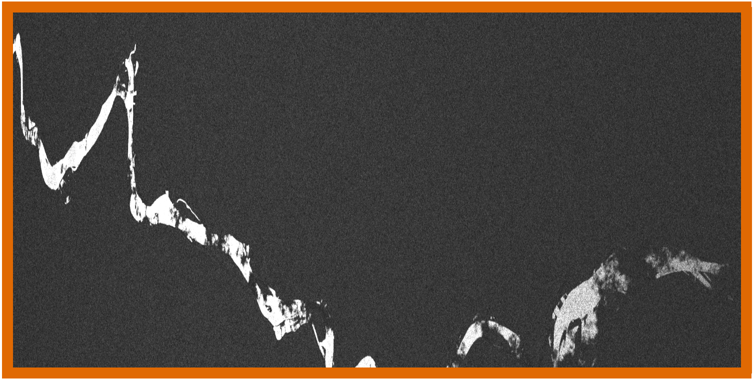

Presence of "dark water"

Results

Camargue Po Kaw

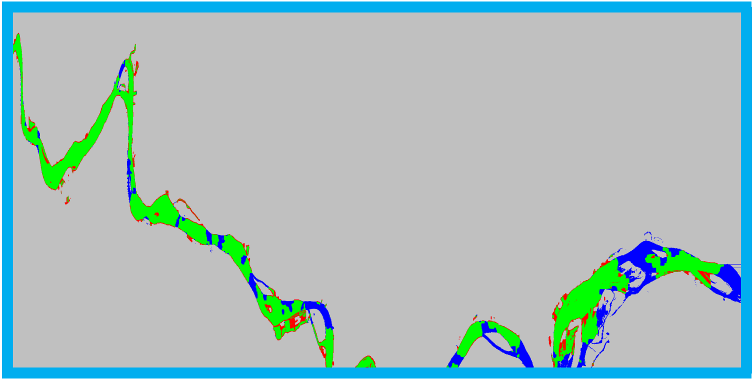

True positive True negative False positive False negative

Results

Camargue Po Kaw

	ML	MAP	MRF Constant	Proposed model
TPR	69.31%	53.67%	71.41%	74.24%
FPR	5.61%	0.34%	0.72%	0.80%
MCC	0.52	0.69	0.77	0.78
ER	119.26%	51.60%	39.95%	38.40%

$$\text{True positive rate: } \mathrm{TPR} = \frac{TP}{TP + FN}$$

$$\text{False positive rate: } \mathrm{FPR} = \frac{FP}{FP + TN}$$

$$\mathrm{MCC} = \frac{TP \times TN - FP \times FN}{\sqrt{(TP + FP)(TP + FN)(TN + FP)(TN + FN)}}$$

$$\text{Error rate: } \mathrm{ER} = \frac{FP + FN}{TP + FN}$$

Results

Camargue Po Kaw

Acquired by airborne sensor SETHI (ONERA): P-band, high incidence angle.

v

Ground truth

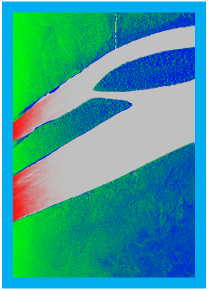

ML

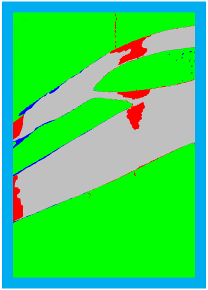

Proposed model

True positive | True negative | False positive | False negative

Results

Camargue Po Kaw

	ML	MAP	MRF Constant	Proposed model
TPR	54.49%	27.99%	79.88%	99.00%
FPR	7.06%	2.85%	7.78%	9.58%
MCC	0.46	0.30	0.68	0.91
ER	48.93%	73.39%	23.90%	5.66%

$$\text{True positive rate: TPR} = \frac{TP}{TP + FN}$$

$$\text{False positive rate: FPR} = \frac{FP}{FP + TN}$$

$$\text{MCC} = \frac{TP \times TN - FP \times FN}{\sqrt{(TP + FP)(TP + FN)(TN + FP)(TN + FN)}}$$

$$\text{Error rate: ER} = \frac{FP + FN}{TP + FN}$$

Conclusion

1st contribution

- Dedicated methods for large but compact objects in SWOT images adapted to specific SWOT characteristics.
- Applicable when antenna pattern can not be inverted or when there are strong local variations in the image.
- Based on a widely-used model, with the addition of parameters estimation.

- Integration in SWOT toolchain.
- Large scale testing in progress.

Sylvain Lobry, Loïc Denis, Florence Tupin, Roger Fjørtoft,
Double MRF for water classification in SAR images by joint detection and reflectivity estimation, IGARSS, USA, 2017.

Conclusion

2nd contribution

A method for the detection of thin elements in SWOT images.
Combination of simple processing steps, with a MRF definition taking into account geometrical priors.

Sylvain Lobry, Florence Tupin, Roger Fjørtoft,
Unsupervised detection of thin water surfaces in SWOT images based on segment detection and connection,IGARSS, USA, 2017.

Outline

Part 1
Water detection in SWOT amplitude images

Part 2
Processing of multi-temporal series of SAR images

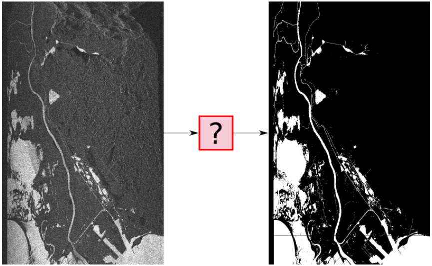

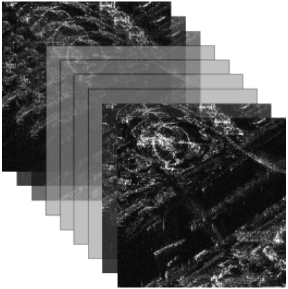

Outline

Part 1
Water detection in SWOT amplitude images

Part 2
Processing of multi-temporal series of SAR images

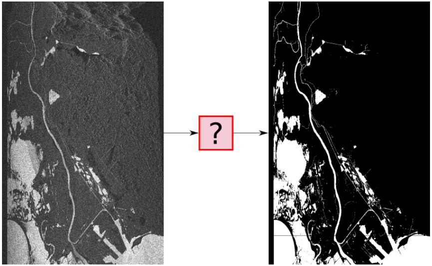

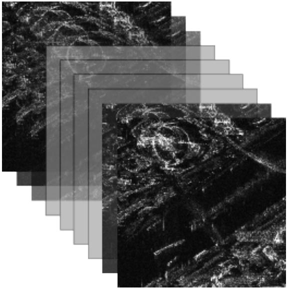

Strong scatterers

With classical SAR systems (e.g. TerraSAR-X (DLR): X-band (9.65GHz), incidence ($\approx 30°$)):

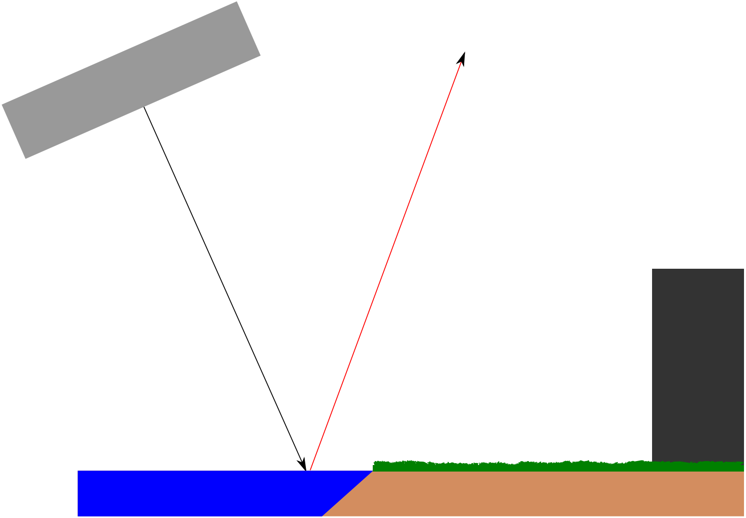

Strong scatterers

With classical SAR systems (e.g. TerraSAR-X (DLR): X-band (9.65GHz), incidence ($\approx 30°$)):

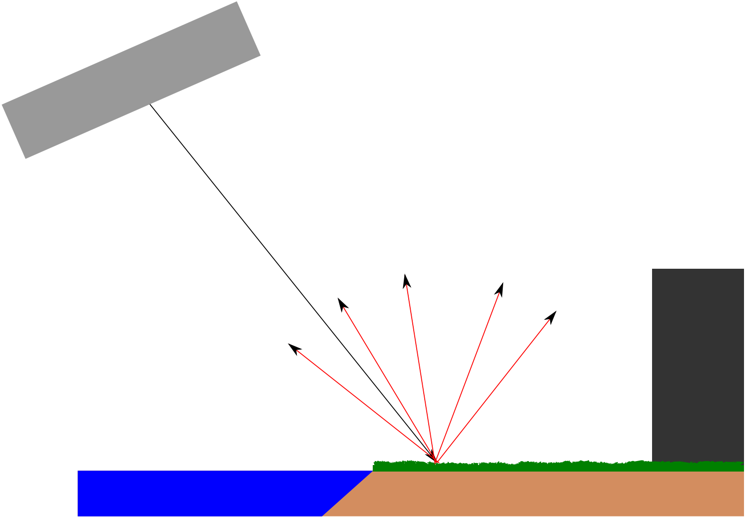

Strong scatterers

With classical SAR systems (e.g. TerraSAR-X (DLR): X-band (9.65GHz), incidence ($\approx 30^\circ$)):

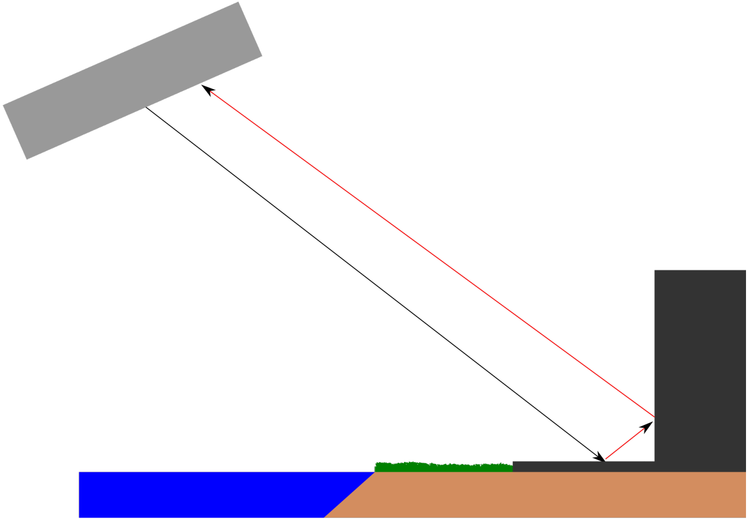

Strong scatterers

With classical SAR systems (e.g. TerraSAR-X (DLR): X-band (9.65GHz), incidence ($\approx 30^\circ$)):

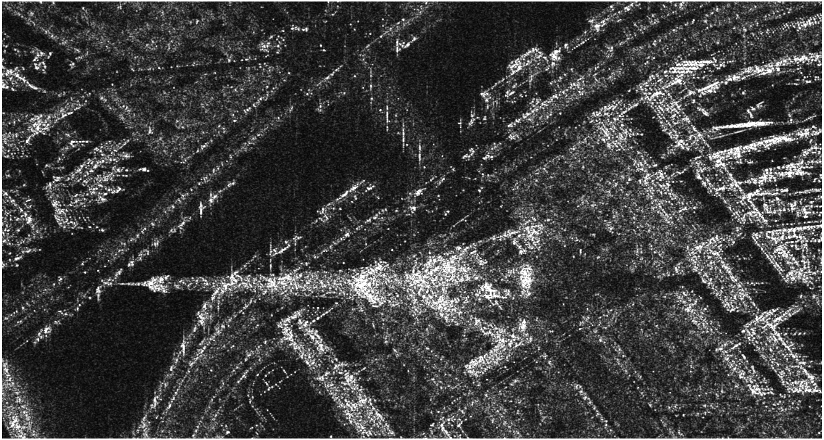

Goal

- Man-made structures $\Rightarrow$ strong scatterers in images.
- Problems: What is a strong scatterer? How to detect it?

Goal

- Man-made structures ⇒ strong scatterers in images.
- Problems: What is a strong scatterer? How to detect it?

Strong scatterer: point with a radiometry at least an order of magnitude higher than its surrounding area.

Model (for one point of the image):

$$\begin{aligned} v_{t,i} &= u_{t,i} \times n_{t,i} \\ &= (b_{t,i} + s_{t,i}) \times n_{t,i} \,, \end{aligned}$$

with $v_{t,i}$ the observation, $b_{t,i}$ the background and $s_{t,i}$ the strong scatterer

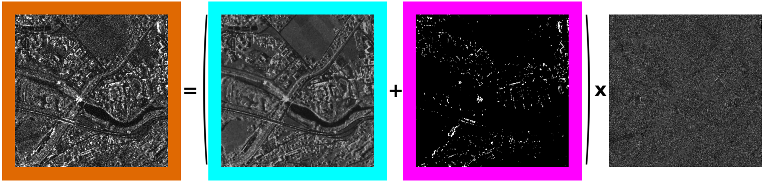

Goal

- Man-made structures $\Rightarrow$ strong scatterers in images.
- Problems: What is a strong scatterer? How to detect it?

Likelihood ratio:

$$\log \frac{p(\{v_{t,i}\}|b_{t,i} + s_{t,i})}{p(\{v_{t,i}\}|b_{t,i} + 0)} \underset{\mathcal{H}_0}{\overset{\mathcal{H}_1}{\gtrless}} \lambda \,.$$

New problem: values for the background $b_{t,i}$ and for the strong scatterer $s_{t,i}$?

Goal

- Man-made structures $\Rightarrow$ strong scatterers in images.
- Problems: What is a strong scatterer? How to detect it?

Values for the background $b_{t,i}$ and for the strong scatterer $s_{t,i}$? We need to know where are the strong scatterers.

Goal

- Man-made structures $\Rightarrow$ strong scatterers in images.
- Problems: What is a strong scatterer? How to detect it?

Proposed solution

Joint resolution [Denis et al., 2010]

- An estimation problem: $b_{t,i}$ and $s_{t,i}$.
- A detection problem: the scatterers $s_{t,i} > 0$ and the changes

Different models:

- Multiple backgrounds + multiple scatterers.
- One background + multiple scatterers.
- One background + multiple scatterers + changes.

Objective

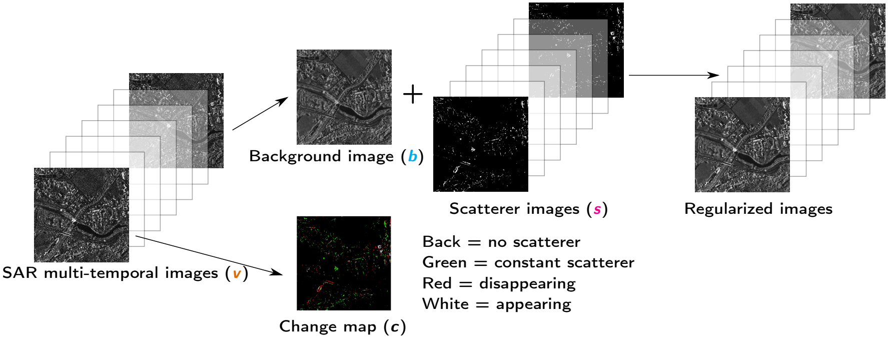

Results on a time-series of TerraSAR-X images of Saint-Gervais, France.
13 images (05/31/09-11/25/2011).
Projects MTH0232, LAN 2708 and LAN1746.

A detection problem

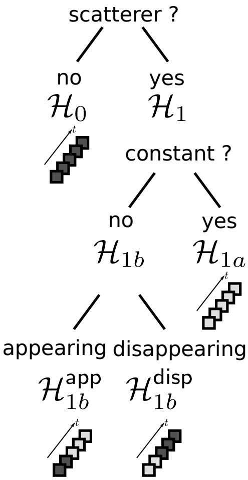

In one point, hierarchical hypothesis test:

- Scatterers detection:
  - Hypothesis "Absence of a scatterer": $\mathcal{H}_0$
  - Hypothesis "Presence of a scatterer": $\mathcal{H}_1$
- Change detection:
  - Hypothesis "Constant scatterer": $\mathcal{H}_{1a}$
  - Hypothesis "Change": $\mathcal{H}_{1b}$

    $\Rightarrow$ "Appearance": $\mathcal{H}_{1b}^{\text{app}}$ at one date $t_{c\,i}$

    $\Rightarrow$ "Disappearance": $\mathcal{H}_{1b}^{\text{disp}}$ at one date $t_{c\,i}$

A detection problem

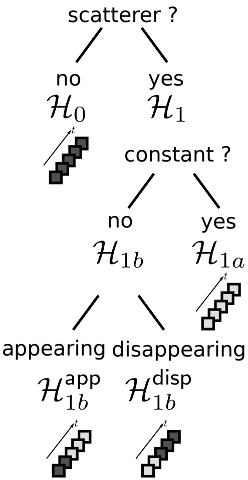

Negative log-likelihood: function of the background and strong scatterers radiometries for each hypothesis:

$$\mathscr{L}_0(b_i) = \sum_t \ell(v_{t,i}, b_i, 0)$$

$$\mathscr{L}_{1a}(b_i, r) = \sum_t \ell(v_{t,i}, b_i, r)$$

$$\mathscr{L}_{1b}^{\text{app}}(b_i, r, t_{c\,i}) = \sum_{t=1}^{t_{c\,i}-1} \ell(v_{t,i}, b_i, 0) + \sum_{t=t_{c\,i}}^{n} \ell(v_{t,i}, b_i, r)$$

$$\mathscr{L}_{1b}^{\text{dis}}(b_i, r, t_{c\,i}) = \sum_{t=1}^{t_{c\,i}-1} \ell(v_{t,i}, b_i, r) + \sum_{t=t_{c\,i}}^{n} \ell(v_{t,i}, b_i, 0)$$

Change detection

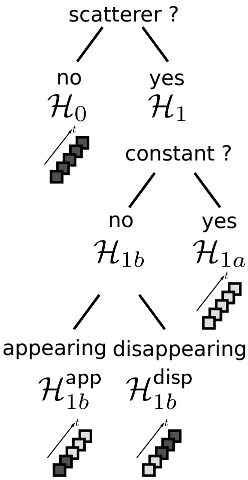

Likelihood-ratio test

$$\log \frac{p(\{v_i\}|\mathcal{H}_{1b})}{p(\{v_i\}|\mathcal{H}_{1a})} \underset{\mathcal{H}_{1a}}{\overset{\mathcal{H}_{1b}}{\gtrless}} \eta \, .$$

For a given r and b_i: most probable date of appearance/disappearance? $\Rightarrow$ GLRT:

$$\widehat{\mathscr{L}_{1b}}(b_i, r) + \eta \underset{\mathcal{H}_{1b}}{\overset{\mathcal{H}_{1a}}{\gtrless}} \mathscr{L}_{1a}(b_i, r) \, ,$$

Change detection

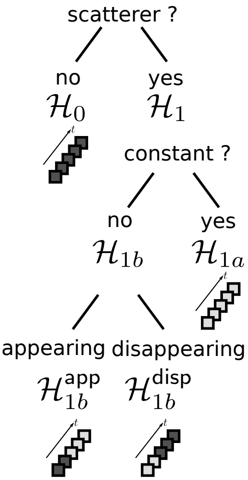

Likelihood-ratio test

$$\log \frac{p(\{v_i\}|\mathcal{H}_{1b})}{p(\{v_i\}|\mathcal{H}_{1a})} \underset{\mathcal{H}_{1a}}{\overset{\mathcal{H}_{1b}}{\gtrless}} \eta\,.$$

with $\widehat{\mathscr{L}_{1b}}(b_i, r)$:

$$\widehat{\mathscr{L}_{1b}}(b_i, r) = \min_{t_{c\,i}} \min\left[\mathscr{L}_{1b}^{\text{app}}(b_i, r, t_{c\,i}),\, \mathscr{L}_{1b}^{\text{dis}}(b_i, r, t_{c\,i})\right].$$

using the estimated values for the background and for the scatterer on the considered dates (depends on $t_{c\,i}$).

Scatterers detection

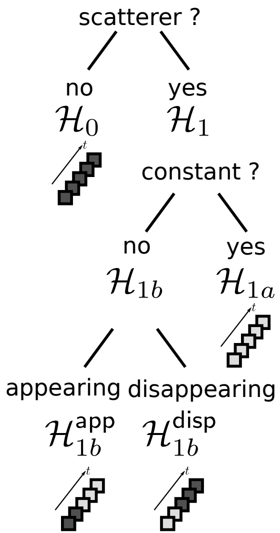

Likelihood ratio test:

$$\log \frac{p(\{v_i\}|\mathcal{H}_1)}{p(\{v_i\}|\mathcal{H}_0)} \underset{\mathcal{H}_0}{\overset{\mathcal{H}_1}{\gtrless}} \lambda\,.$$

Maximum likelihood estimate for the radiometry of the strong scatterer $\Rightarrow$ GLRT:

$$\widehat{\mathscr{L}_1}(b_i) + \lambda \underset{\mathcal{H}_1}{\overset{\mathcal{H}_0}{\gtrless}} \mathscr{L}_0(b_i)\,,$$

with:

$$\widehat{\mathscr{L}_1}(b_i) = \min_r \min\left[\mathscr{L}_{1a}(b_i, r),\ \widehat{\mathscr{L}_{1b}}(b_i, r) + \eta\right].$$

Optimal value for the strong scatterer

Maximum likelihood estimate (Rayleigh distribution) for the different scenarios:

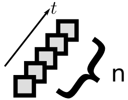

$$r = \left[\sqrt{\frac{1}{n} \sum_{t} {v_i}^2} - b_i \right]^+ ,$$

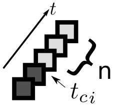

$$r = \left[\sqrt{\frac{1}{n} \sum_{t=t_{ci}}^{t_{ci}+n} {v_i}^2} - b_i \right]^+ ,$$

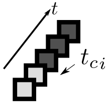

$$r = \left[\sqrt{\frac{1}{n} \sum_{t=1}^{t_{ci}} {v_i}^2} - b_i \right]^+ ,$$

Background radiometry estimation

Negative log-likelihood of the background:

$$\widehat{\mathscr{L}}(b_i) = \min\left[\mathscr{L}_0(b_i),\, \widehat{\mathscr{L}_1}(b_i) + \lambda\right].$$

Prior: Piecewise-constant background $\Rightarrow$ *Total variation* (TV):

$$-\log p(\boldsymbol{b}) = \mu \sum_{i \sim j} |b_i - b_j| \equiv \mu\, \mathrm{TV}(\boldsymbol{b})\,,$$

Maximum a posteriori estimation:

$$\hat{\boldsymbol{b}} = \underset{\boldsymbol{b} \in \mathbb{R}^m}{\arg\min} \sum_i \widehat{\mathscr{L}}(b_i) + \mu\, \mathrm{TV}(\boldsymbol{b})\,,$$

$$\text{such that} \quad \boldsymbol{b} \geq 0$$

MAP model

$$\mathop{\arg\min}_{\substack{(\boldsymbol{d},\boldsymbol{c},\boldsymbol{a})\in\{0,1\}^{m\times 3}\\ \boldsymbol{b}\in\mathbb{R}^m\\ \boldsymbol{r}\in\mathbb{R}^m\\ \boldsymbol{s}\in\mathbb{R}^{m\times n}\\ \boldsymbol{t_c}\in\{2,\ldots,n\}^m}} \sum_{i,t} \ell(v_i, b_i, s_{t,i}) + \lambda\,\|\boldsymbol{d}\|_0 + \eta\,\|\boldsymbol{c}\|_0 + \mu\,\mathrm{TV}(\boldsymbol{b})$$

$$\text{such that}\quad \begin{array}{lrcl}
\forall i,\ \forall t, & (d_i - 1)\cdot s_{t,i} & = & 0\\
\forall i,\ \forall t, & (c_i - 1)\cdot (s_{t,i} - r) & = & 0\\
\forall i,\ \forall t < t_{c\,i}, & c_i \cdot a_i \cdot s_{t,i} & = & 0\\
\forall i,\ \forall t \geq t_{c\,i}, & c_i \cdot a_i \cdot (s_{t,i} - r) & = & 0\\
\forall i,\ \forall t < t_{c\,i}, & c_i \cdot (1 - a_i)\cdot (s_{t,i} - r) & = & 0\\
\forall i,\ \forall t \geq t_{c\,i}, & c_i \cdot (1 - a_i)\cdot s_{t,i} & = & 0\\
\forall i, & b_i & \geq & 0\\
\forall i, & r & \geq & 0
\end{array}$$

with $d_i = 1$: scatterer at i, and c_i: change at i.

Optimization

2-steps resolution:

- Optimal values for the strong scatterers given a fixed background: $\widehat{s_{t,i}(b_i)}$ (Hierarchical hypothesis tests)
- Sub-problem:

$$\sum_{i,t} \ell(v_i, b_i, \widehat{s_{t,i}(b_i)}) + \lambda \, \|\widehat{\boldsymbol{d}(\boldsymbol{b})}\|_0$$

$$+\eta \, \|\widehat{\boldsymbol{c}(\boldsymbol{b})}\|_0 + \mu \, \mathrm{TV}(\boldsymbol{b})$$

- Sum of separable terms depending on $\boldsymbol{b}$ + pair-wise convex prior $\Rightarrow$ graph-cut optimization

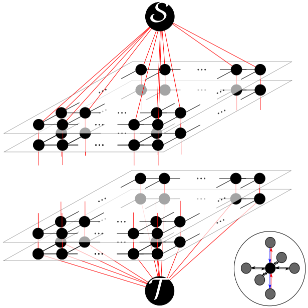

Graph construction based on [Ishikawa, 2003].

Results

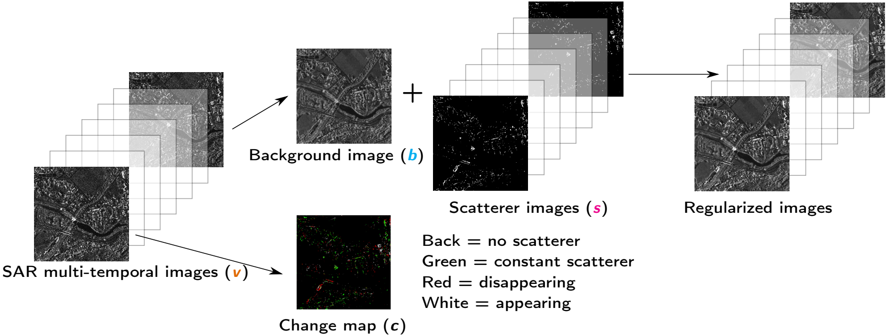

Results on a time-series of TerraSAR-X images of Saint-Gervais, France.
13 images (05/31/09-11/25/2011).
Projects MTH0232, LAN 2708 and LAN1746.

Results

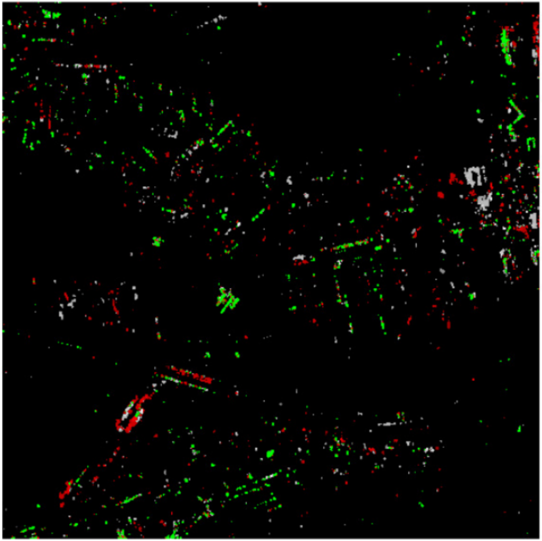

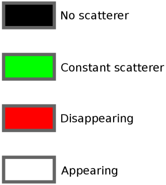

Results

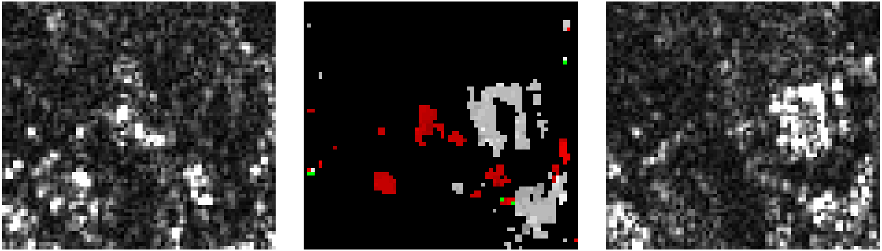

No scatterer

Constant scatterer

Disappearing

Appearing

Results

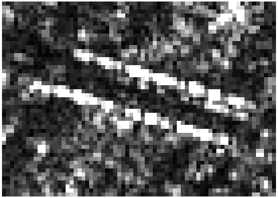

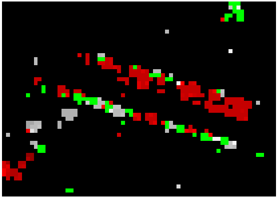

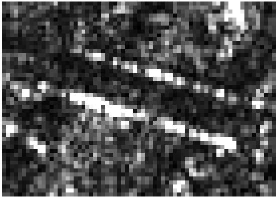

No scatterer

Constant scatterer

Disappearing

Appearing

Conclusion

3rd contribution

Model for regularization, scatterers detection and change detection for SAR urban time series.

- Semi-automatic parameters tuning.
- Exact optimization.
- Only one model presented: several variants studied.

Sylvain Lobry, Loïc Denis, Florence Tupin, Weiying Zhao,
Décomposition de séries temporelles d'images SAR pour la détection de changement,
Traitement du Signal (GRETSI, Lavoisier)

Sylvain Lobry, Loïc Denis, Florence Tupin,
Multi-temporal SAR image decomposition into strong scatterers, background, and speckle, IEEE JSTARS, 2016

Conclusion

- Water detection:
  - two models to estimate variable parameters (Region-based and Markovian).
  - Thin-elements detection.
- Multi-temporal urban SAR processing:
  - model for time-series regularization.
  - Model for strong scatterers detection.
  - Model for change detection.
- Similarities for the data (SAR) and the models (MRF)
  $\Rightarrow$ Transferable techniques:
  - sub-optimal but tractable MRF optimization.
  - Multi-temporal processing can be adapted to SWOT.

Perspectives (water detection)

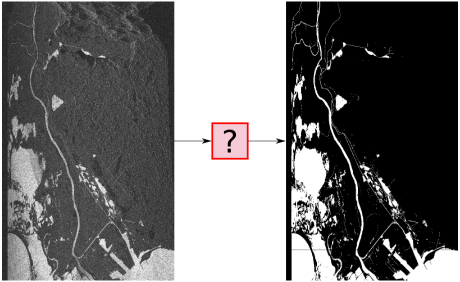

- Classification: extend Ising to 3D.
- Parameters estimation: how to take into account multi-temporal series?
  - Quadratic terms between pixels at different dates?
  - Take previous parameters map as initialization?

Perspectives (Multi-temporal processing)

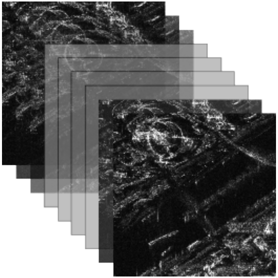

- Use Rice likelihood when strong scatterers are present.
- Influence of the sampling and apodisation.
- Change detection model:
  - Not the same probability of change detection w.r.t. time: *under study*.
  - Only one change per pixel: *possible, but direct extension intractable*.
  - Allow for changes in the background.

Selected publications

International journal:

- Sylvain Lobry, Loïc Denis, Florence Tupin,
  Multi-temporal SAR image decomposition into strong scatterers, background, and speckle, IEEE JSTARS, 2016

National journal:

- Sylvain Lobry, Loïc Denis, Florence Tupin, Weiying Zhao,
  Décomposition de séries temporelles d'images SAR pour la détection de changement, Traitement du Signal (GRETSI, Lavoisier) (accepted)

International conferences (total: 6):

- Sylvain Lobry, Loïc Denis, Florence Tupin, Roger Fjørtoft,
  Double MRF for water classification in SAR images by joint detection and reflectivity estimation, IGARSS, USA, 2017.
- Sylvain Lobry, Florence Tupin, Roger Fjørtoft,
  Unsupervised detection of thin water surfaces in SWOT images based on segment detection and connection, IGARSS, USA, 2017.
- Sylvain Lobry, Florence Tupin, Loïc Denis,
  A decomposition model for scatterers change detection in multi-temporal series of SAR images. IGARSS, China, 2016.

National conferences (total: 2)

Compact object detection | Thin elements detection | Decomposition models

Thank you!

References

- Ben Ayed, I., Mitiche, A., and Belhadj, Z. (2005).
  Multiregion level-set partitioning of synthetic aperture radar images.
  Pattern Analysis and Machine Intelligence, IEEE Transactions on, 27(5):793–800.

- Cao, F., Tupin, F., Nicolas, J.-M., Fjørtoft, R., and Pourthié, N. (2011).
  Extraction of water surfaces in simulated Ka-band SAR images of KaRIn on SWOT.
  In *Geoscience and Remote Sensing Symposium (IGARSS), 2011 IEEE International*, pages 3562–3565.

- Cazals, C., Rapinel, S., Frison, P.-L., Bonis, A., Mercier, G., Mallet, C., Corgne, S., and Rudant, J.-P. (2016).
  Mapping and characterization of hydrological dynamics in a coastal marsh using high temporal resolution sentinel-1a images.
  Remote Sensing, 8(7):570.

- Deledalle, C.-A., Denis, L., Tupin, F., Reigber, A., and Jäger, M. (2015).
  NL-SAR: A Unified Nonlocal Framework for Resolution-Preserving (Pol)(In)SAR Denoising.
  Geoscience and Remote Sensing, IEEE Transactions on, 53(4):2021–2038.

References (cont.)

- Denis, L., Tupin, F., and Rondeau, X. (2010).
  Exact discrete minimization for TV+L0 image decomposition models.
  In *Image Processing (ICIP), 2010 17th IEEE International Conference on*, pages 2525–2528. IEEE.
- Fjørtoft, R., Lopes, A., Marthon, P., and Cubero-Castan, E. (1998).
  An optimal multiedge detector for SAR image segmentation.
  Geoscience and Remote Sensing, IEEE Transactions on, 36(3):793–802.
- Goodman, J. W. (2007).
  Speckle phenomena in optics: theory and applications.
  Roberts and Company Publishers.
- Greig, D. et al. (1989).
  Exact maximum a posteriori estimation for binary images.
  Journal of the Royal Statistical Society. Series B (Methodological), pages 271–279.

References (cont.)

- Ishikawa, H. (2003).
  Exact optimization for Markov random fields with convex priors.
  Pattern Analysis and Machine Intelligence, IEEE Transactions on, 25(10):1333–1336.

- Lee, J.-S. (1981).
  Speckle analysis and smoothing of synthetic aperture radar images.
  Computer graphics and image processing, 17(1):24–32.

- Liu, H. and Jezek, K. (2004).
  A complete high-resolution coastline of antarctica extracted from orthorectified radarsat sar imagery.
  Photogrammetric Engineering & Remote Sensing, 70(5):605–616.

- Perona, P. and Malik, J. (1990).
  Scale-space and edge detection using anisotropic diffusion.
  pattern analysis and machine intelligence, IEEE Transactions on, 12(7):629–639.

References (cont.)

- Silveira, M. et al. (2009).
  Separation Between Water and Land in SAR Images Using Region-Based Level Sets.
  IEEE Geoscience and Remote Sensing Letters, 6(3):471–475.
- Touzi, R., Lopes, A., and Bousquet, P. (1988).
  A statistical and geometrical edge detector for SAR images.
  geoscience and remote sensing, IEEE Transactions on, 26(6):764–773.

Radiometry vs Wind

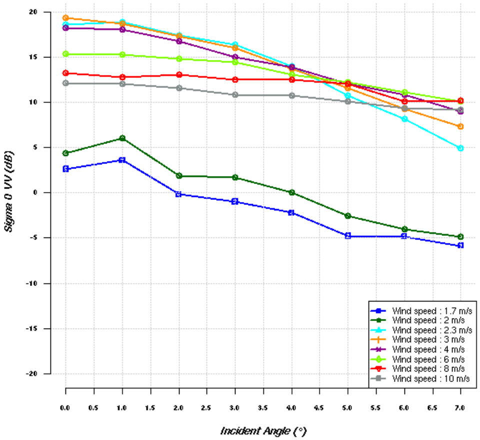

R. Fjørtoft, J.-M. Gaudin, N. Pourthié, J.-C. Lalaurie, A. Mallet, J.-F. Nouvel, J. Martinot-Lagarde, H. Oriot, P. Borderies, C. Ruiz, and S. Daniel,

"KaRIn on SWOT: Characteristics of Near-nadir Ka-band Interferometric SAR Imagery",

IEEE Transactions on Geoscience and Remote Sensing, Vol. 52, No. 4, April 2014.

Sub-optimal optimization

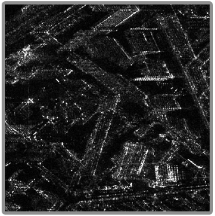

Input

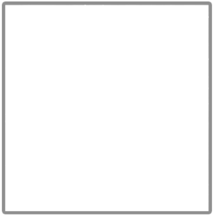

Output

Optimization - MRF Ising

- Graphcut from [Greig et al., 1989]:
  - + optimal.
  - + Fast.
  - − Memory required.
- ICM (greedy algorithm):
  - + fast.
  - − Local minimum.
- Convex relaxation + TV $\Rightarrow$ proximal method.

Optimization - MRF Parameters

- Conjugate gradients:
  - + converges "quickly"
  - + Considered efficient in the case of quadratic functions.
  - − Convergence parameters to tune.
- Proximal method could also be used (generally adapted to non-smooth functions, e.g. TV or L1)

Optimization - Decomposition

- Graphcut (from [Ishikawa, 2003]):
  - + optimal.
  - – Quantized problem.
  - – Memory required.
- Descent algorithm or proximal methods for a convex relaxation of the prior (i.e. relaxing L0 to L1):
  - – convex relaxation.
  - – Data term is still not convex.
  - – Performances decrease (at least for the strong scatterers detection):

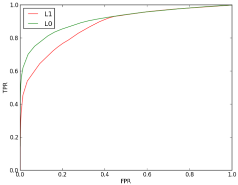

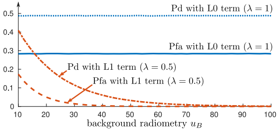

General toolchain

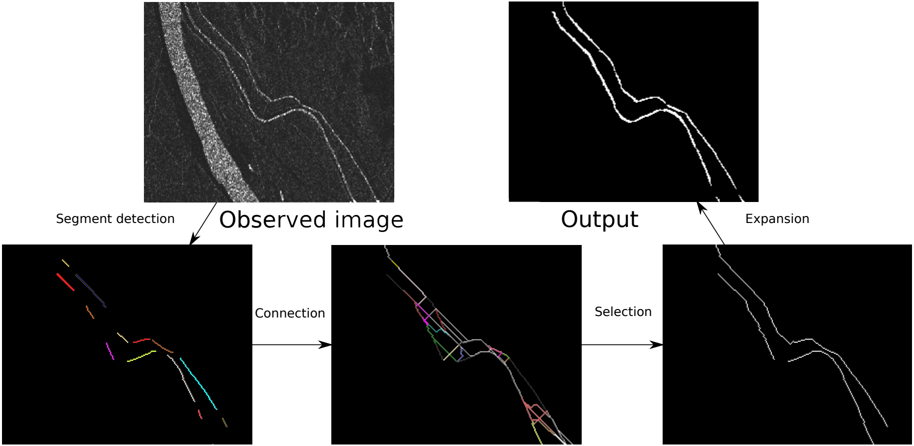

General toolchain

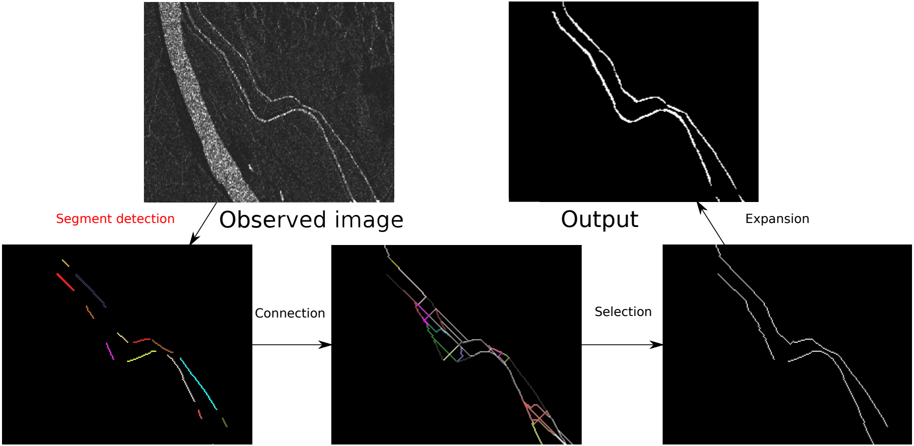

General toolchain

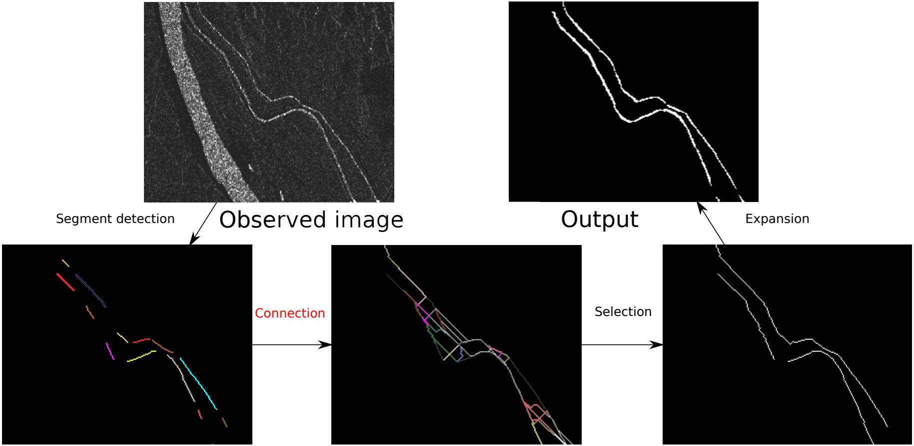

General toolchain

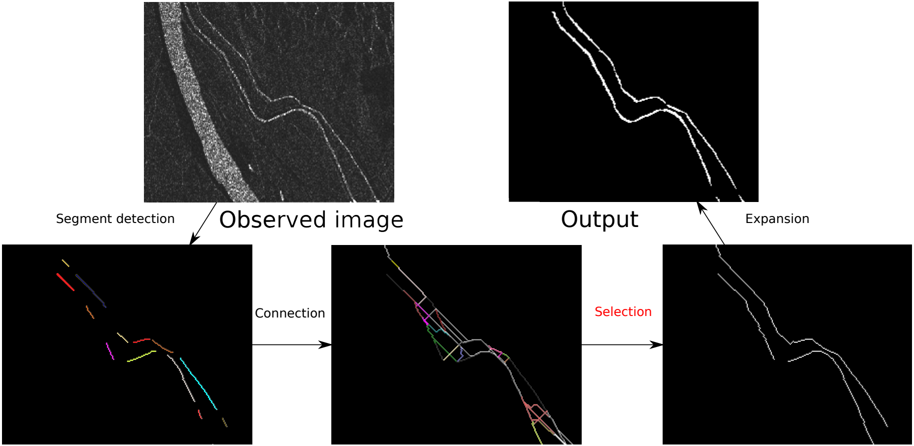

General toolchain

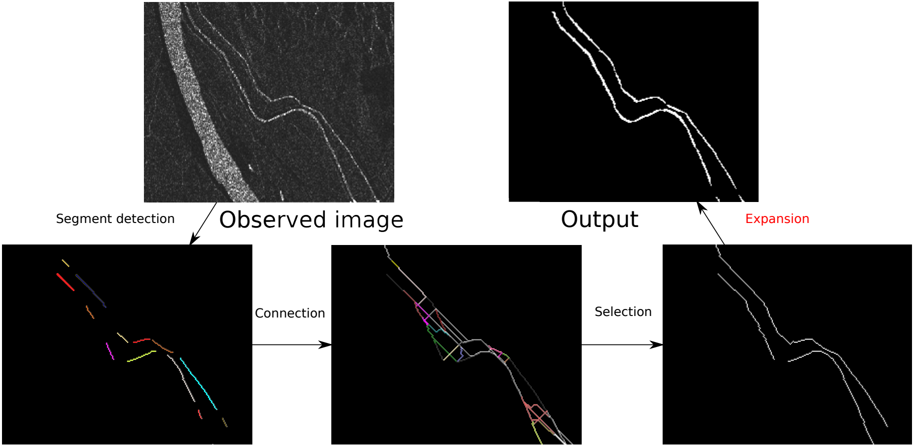

General toolchain

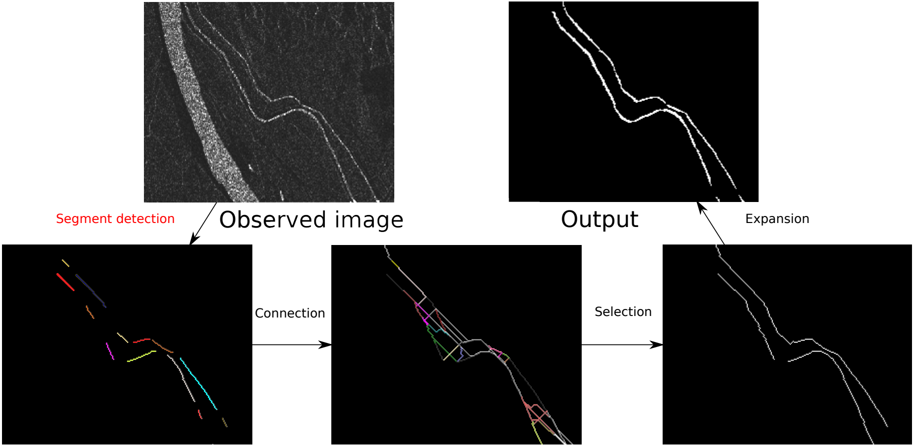

Segment detection

- Pixel level detector: for each pixel:
  - does it belong to a segment ?
  - which width ?
  - which orientation ?
- Comparison between the rectangle characterizing the segment and adjacent ones.

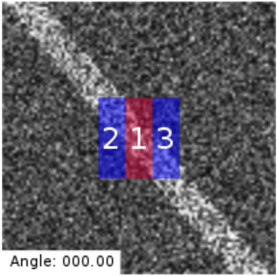

Segment detection

Score for a given rectangle r_1 (red in picture):

$$D1(r_1) = 1 - \max\left(\min\left(\frac{\mu_{r_1}}{\mu_{r_2}}, \frac{\mu_{r_2}}{\mu_{r_1}}\right), \min\left(\frac{\mu_{r_1}}{\mu_{r_3}}, \frac{\mu_{r_3}}{\mu_{r_1}}\right)\right)$$

where μ_{r_x} is the mean reflectivity in the rectangle r_x given by the MLE.

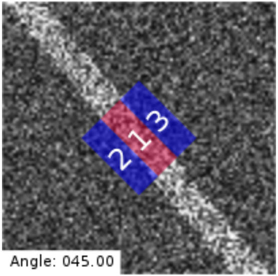

$$D2(r_1) = \min\left(cc(r_1, r_2), cc(r_1, r_3)\right)$$

where $cc(r_1, r_2)$ is the discrete normalized cross-correlation between r_1 and r_2.

$$D1D2(r_1) = \frac{\overline{D1}(r_1)\overline{D2}(r_1)}{1 - \overline{D1}(r_1) - \overline{D2}(r_1) + 2\overline{D1}(r_1)\overline{D2}(r_1)},$$

where $\overline{x}(r)$ is the score $x(r)$ centered between $[0, 1]$.

Segment detection

For each pixel i: $l_i = \max_{r \in \mathcal{R}_i} D1D2(r)$. Then post-process:

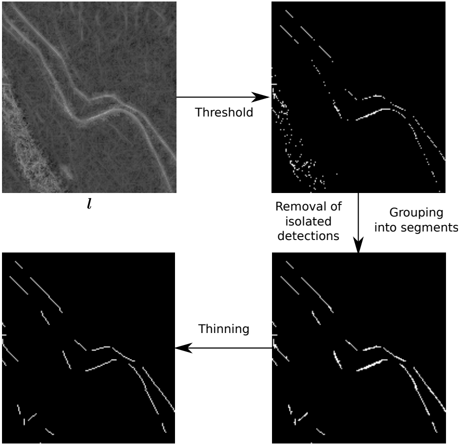

General toolchain

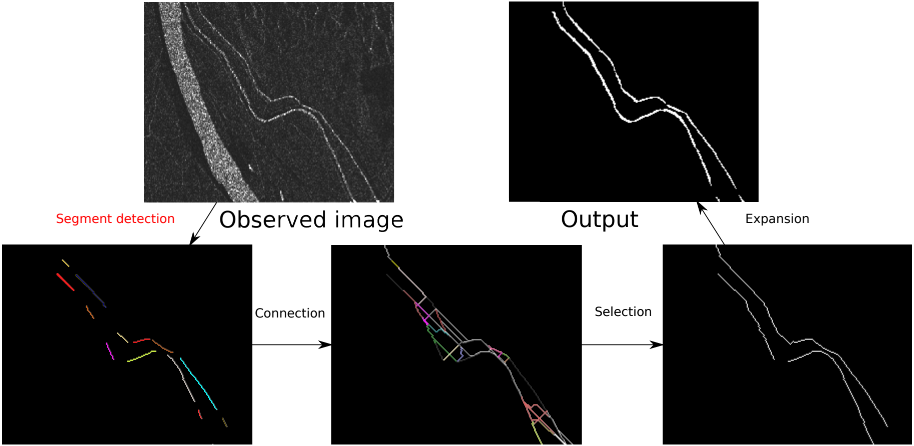

General toolchain

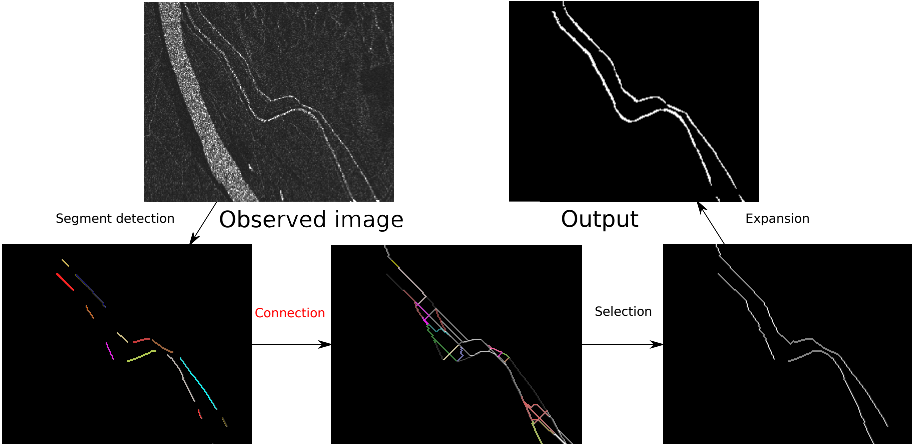

Connection

Connect segments using Dijkstra's algorithm:

- Find shortest path between two nodes on a graph (greedy $\Rightarrow$ local minimum).
- Graph construction:
  - Nodes = pixels
  - Weight from a to $b = 1 - I_b$.

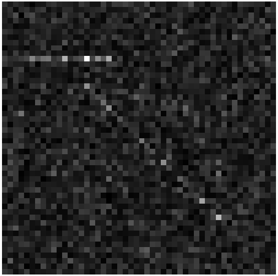

Noisy Image

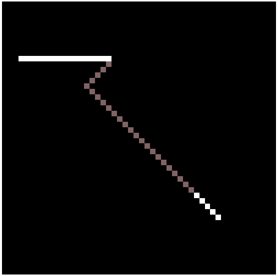

Ground truth

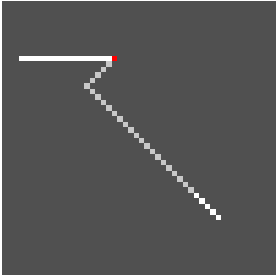

Dijkstra algorithm

Connection

Connect segments using Dijkstra's algorithm:

- Find shortest path between two nodes on a graph (greedy $\Rightarrow$ local minimum).
- Graph construction:
  - Nodes = pixels
  - Weight from a to $b = 1 - I_b$.

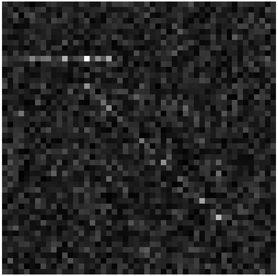

Noisy Image

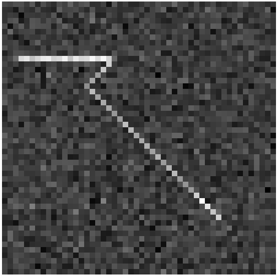

I

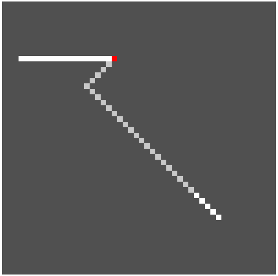

Dijkstra algorithm

Connection

Connect segments using Dijkstra's algorithm:

- Find shortest path between two nodes on a graph (greedy $\Rightarrow$ local minimum).
- Graph construction:
  - Nodes = pixels
  - Weight from a to $b = 1 - I_b$.

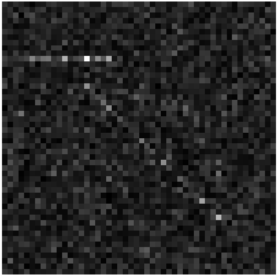

Noisy Image

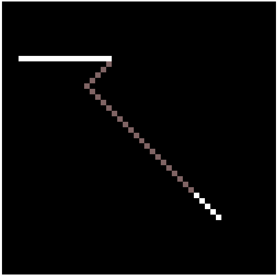

Ground truth

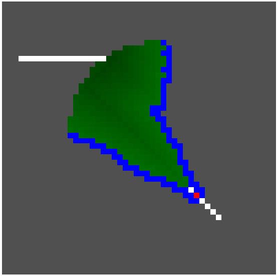

Dijkstra algorithm

Connection

- High complexity ($O(|N| \log |N|)$) where N is the number of possible pixels for the connection $\Rightarrow$
  - Restrict space search.
  - Restrict to "close" segments.

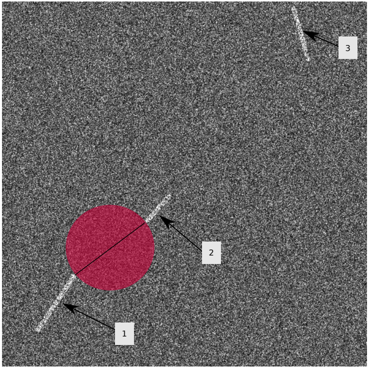

General toolchain

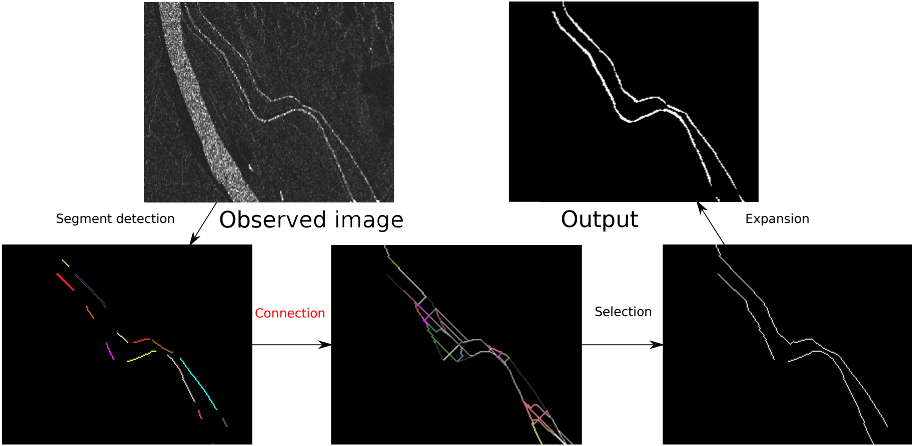

General toolchain

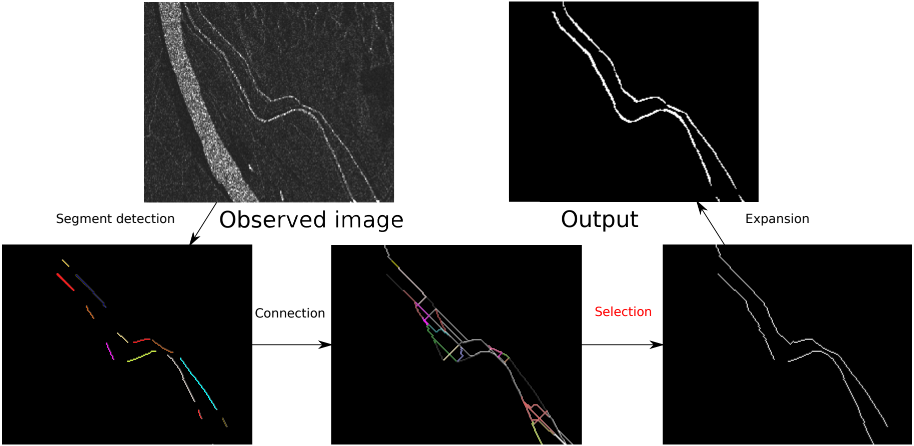

Selection

- Goal: select connections based on:
  - Cost ($\propto$ probability of being water).
  - Contribution to general properties of river networks.
- find labeling $\boldsymbol{x}$ of connections $\mathcal{C}$:

$$\forall c \in \mathcal{C}\,, \qquad x_c = \begin{cases} 1 & \text{if } c \text{ belongs to the network} \\ 0 & \text{otherwise} \end{cases}$$

- $\Rightarrow$ minimize:

$$\begin{aligned} \hat{\boldsymbol{x}} &= \arg\min_{\boldsymbol{x}} \mathcal{E}(\boldsymbol{x}) \\ &= DT(\boldsymbol{I}, \boldsymbol{x}) - \log(p(\boldsymbol{x}))\,. \end{aligned}$$

Selection - Data term

$$\hat{\boldsymbol{x}} = DT(\boldsymbol{I}, \boldsymbol{x}) - \log(p(\boldsymbol{x}))\,.$$

Cost for the selected connection from the normalized value (detection step).

$$DT(\boldsymbol{I}, \boldsymbol{x}) = \sum_{c \in \mathcal{C}} DT(\boldsymbol{I}, x_c)\,,$$

with:

$$DT(\boldsymbol{I}, x_c) = \begin{cases} \frac{1}{|c|} \sum_{i \in c} (1 - I_i) & \text{if } x_c = 1 \\ 0 & \text{otherwise.} \end{cases}$$

Selection - prior

$$\hat{\boldsymbol{x}} = DT(\boldsymbol{I}, \boldsymbol{x}) - \log(p(\boldsymbol{x}))\,.$$

Sum of 6 terms enforcing global river networks properties:

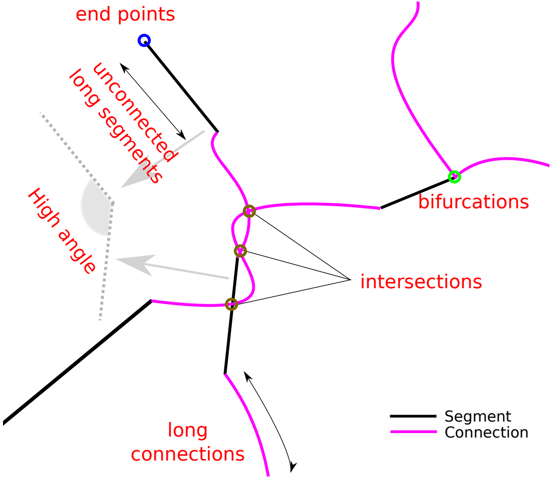

General toolchain

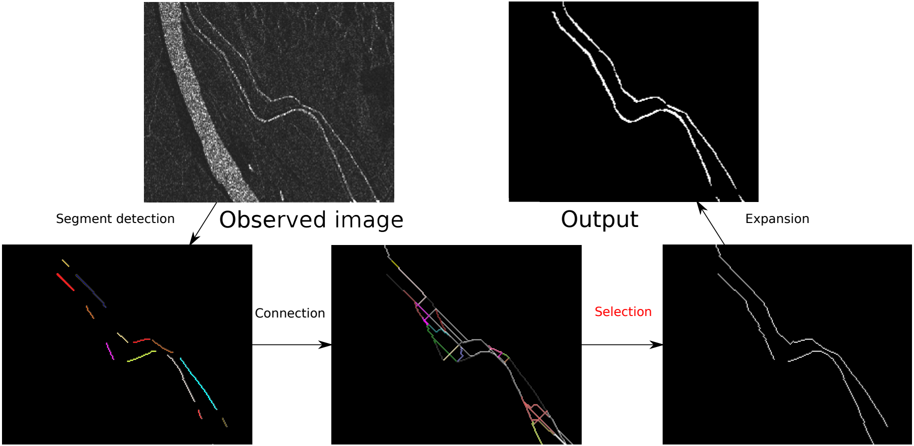

General toolchain

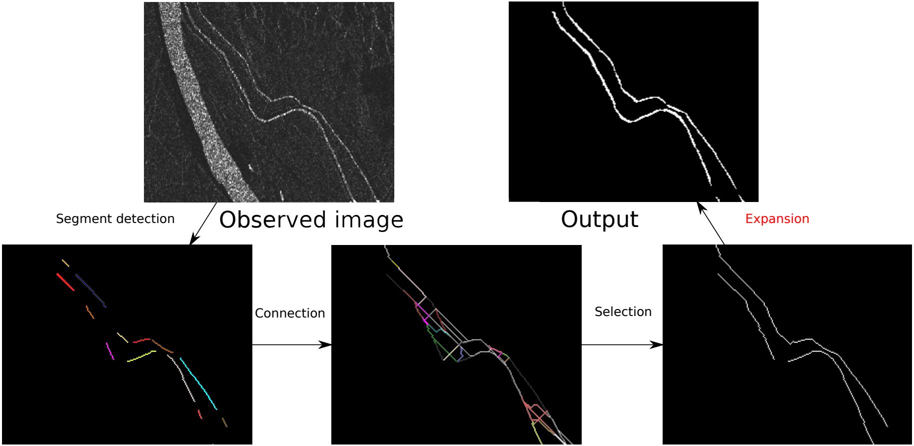

Expansion

- From 1-pixel width detection to pixel-based detection.
- Simple approach based on denoising of a selected area (using NL-SAR [Deledalle et al., 2015]).
- Each connected component in river network is locally denoised, thresholded, and the connected components intersecting are selected.

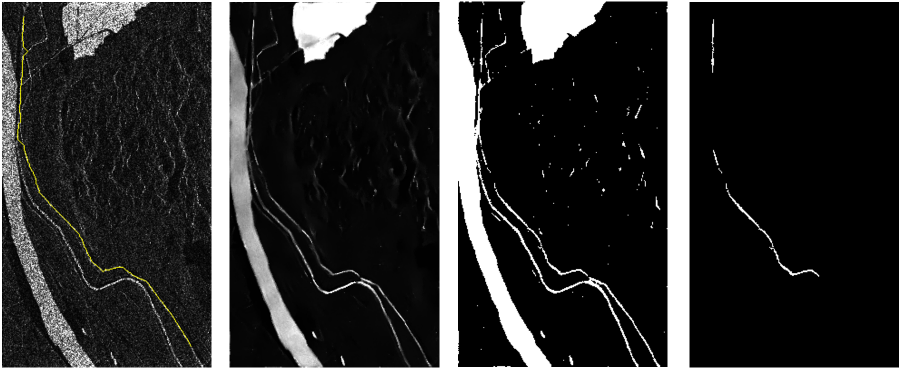

Input | Denoised | Thresholded | Output

Éstimation locale par région

- Définition itérative de la partition.
- Régions doivent être:
  - Assez grandes (pour que l'estimation soit bonne).
  - Assez petites (pour capturer les variations).
- Partitionnement selon quad-tree.
- Paramètres estimés localement dans chaque région.
- Régularisation par rapport aux paramètres théoriques pour éviter des cas divergents.

Éstimation locale par région

$\boldsymbol{v}$

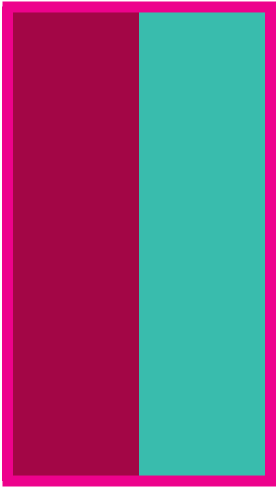

partition 0

Éstimation locale par région

$\boldsymbol{v}$

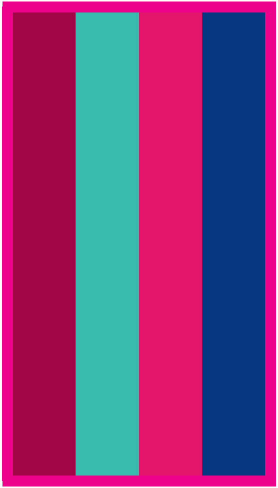

partition 1

Éstimation locale par région

v

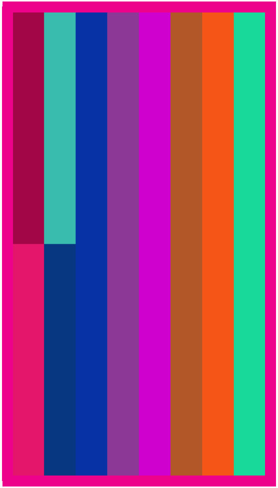

partition 2

ROC on change detection

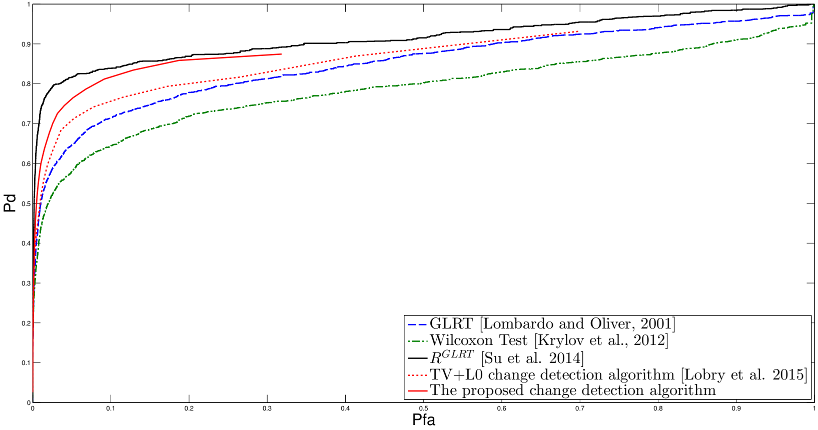

ROC curve of the change detection on Saint-Gervais.

Taking into account multiples changes

$$\widehat{\mathscr{L}_{1b}}(b_i, r) = \min_{t_{c\,i}} \min\left[\mathscr{L}_{1b}^{\text{app}}(b_i, r, t_{c\,i}),\ \mathscr{L}_{1b}^{\text{dis}}(b_i, r, t_{c\,i})\right].$$

- Whereas r can be known analytically (and in constant time when properly implemented), $\min_{t_{c\,i}}$ is linear w.r.t. number of dates.
- If we want two changes:

$$\widehat{\mathscr{L}_{1b}}(b_i, r) = \min_{t_{c\,i1}} \min\Big[\mathscr{L}_{1b}^{\text{app}}(b_i, r, t_{c\,i1}),\ \mathscr{L}_{1b}^{\text{dis}}(b_i, r, t_{c\,i1}) \\ \min_{t_{c\,i2}}\left[\mathscr{L}_{1b}^{\text{app}}(b_i, r, t_{c\,i1}, t_{c\,i2}),\ \mathscr{L}_{1b}^{\text{dis}}(b_i, r, t_{c\,i1}, t_{c\,i2})\right]\Big].$$

  $\Rightarrow$ quadratic on the number of dates.
- Also, still the problem on 3+ changes.
- Should be possible linearly with omnibus tests (e.g. Conradsen et al., Determining the Points of Change in Time Series of Polarimetric SAR Data, TGRS 2016) linearly.
- Clustering